Journal of Mathematical Biology (2024) 88:16
https://doi.org/10.1007/s00285-023-02036-x

Mathematical Biology

A Lifshitz–Slyozov type model for adipocyte size dynamics: limit from Becker–Döring system and numerical simulation

Léo Meyer[1] · Magali Ribot[1] · Romain Yvinec[2,3]

Received: 7 March 2023 / Revised: 4 December 2023 / Accepted: 10 December 2023 /
Published online: 17 January 2024

Abstract

Biological data show that the size distribution of adipose cells follows a bimodal distribution. In this work, we introduce a Lifshitz–Slyozov type model, based on a transport partial differential equation, for the dynamics of the size distribution of adipose cells. We prove a new convergence result from the related Becker–Döring model, a system composed of several ordinary differential equations, toward mild solutions of the Lifshitz–Slyozov model using distribution tail techniques. Then, this result allows us to propose a new advective–diffusive model, the second-order diffusive Lifshitz–Slyozov model, which is expected to better fit the experimental data. Numerical simulations of the solutions to the diffusive Lifshitz–Slyozov model are performed using a well-balanced scheme and compared to solutions to the transport model. Those simulations show that both bimodal and unimodal profiles can be reached asymptotically depending on several parameters. We put in evidence that the asymptotic profile for the second-order system does not depend on initial conditions, unlike for the transport Lifshitz–Slyozov model.

Keywords Adipose cells · Mathematical modeling · Partial differential equations · Stationary solutions · Numerical simulations

Mathematics Subject Classification 92-10 Mathematical modeling or simulation for problems pertaining to biology

✉ Léo Meyer
leo.meyer@math.cnrs.fr

1 Institut Denis Poisson, Université d'Orléans, Orléans, France

2 Inria, Centre Inria de Saclay, Université Paris-Saclay, Palaiseau, France

3 PRC, INRAE, CNRS, Université de Tours, Nouzilly, France

1 Introduction

White adipose tissue is mainly composed of cells, called adipocytes, which store lipids in the body under the form of triglyceride droplets. Experiments in most animals (Jo et al. 2009, 2012; Soula et al. 2013) show that the size distribution of adipocytes follows a striking bimodal distribution with a peak of large amplitude for small adipocytes around the minimal radius, see Fig. 1. The changes in volume of an adipocyte are governed by two opposite phenomena: lipogenesis, that is to say size increase by triglyceride intake, and lipolysis, that is to say size decrease through the hydrolization of triglycerides and the excretion of fatty acids. Modeling the dynamics of size evolution of adipocytes is of great interest in order to study metabolic disorders, such as obesity or type 2 diabetes. Correlation between such diseases and the size and metabolism of adipose cells has been well established in the biological literature. Indeed, in Varlamov et al. (2010), authors show that the size of an adipose cell has a strong correlation with its insulin sensitivity. As such, large cells are less sensitive, therefore a higher body weight leads to greater risks of type 2 diabetes. This study also shows that adipose tissue are very heterogeneous in terms of size of cells. Those findings have also been described in Lee et al. (2019), where the authors show that the adipose tissue is composed of cells that are different both molecularly and phenotypically.

Some computational models have also been used to provide insights into the adipose tissue physiology. In Kim et al. (2008), the authors use an ODE model to investigate the role of lipases in the biochemistry of lipids. They are able to show that determining the active metabolic subdomain in the tissue is the key for accurate simulations, as well as the different activation rates of lipases for diglyceride and triglyceride breakdown. The rate of lipid turnover has also been studied in Arner et al. (2019), where a decrease of the lipid release rate is correlated with the age of the individual. Finally, there are strong links between the adipose tissue and its extracellular matrix, and in case of obesity, one may observe tissue fibrosis such as described in Divoux and Clement (2011). In Peurichard et al. (2017, 2019), adipose tissue is modeled by a 2D agent-based model which takes into account the mechanical interactions between adipose cells and fibers forming the extra-cellular matrix. The authors study the spatial distribution of adipocytes under the form of lobules or in the case of tissue regeneration.

However, only a few mathematical models have been proposed in order to describe the size dynamics of adipose cells and no previous work has tackled a mechanistic understanding of the bimodal feature of adipocyte size distribution.

A first model has been derived by Jo, Periwal et al. Jo et al. (2015, 2012) using a PDE for the adipose cell growth with a phenomenological cell growth rate. They are able to recover the bimodal feature of distributions as well as to perform some curve fitting on biological data. In Soula et al. (2013) and later in Soula et al. (2015), the authors describe the velocity of size change of adipocytes by biological considerations for lipogenesis and lipolysis, leading thus to some transport PDE models. They obtain bimodal distributions by using stochastic variations of the parameters. In Gilleron et al. (2020), the authors perform the analysis and numerical simulations for a size-structured model describing the evolution of a set of adipocytes, including the creation of new adipocytes through differentiation processes from mesenchymal cells

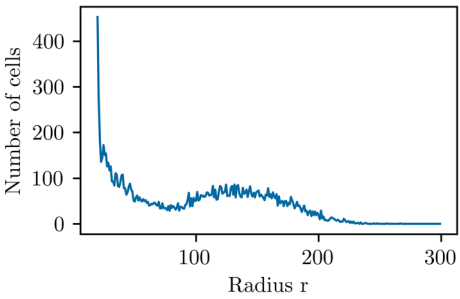

Fig. 1 Example of the distribution of adipocytes in a rat biopsy. Credits: H. Soula

and preadipocytes, and accounting for a size velocity inversely proportional to the total surface of adipocytes. Finally, in Prana et al. (2019), authors use an ODE model to investigate interplay and feedback loop between inflammatory response of bigger adipose cells and the immune system, which may lead to type 2 diabetes. The size of adipocytes is updated at each time step according to some probability of swelling and by a factor depending on the surplus of calories intake. However they do not concern themselves with the size distribution but with the whole tissue inflammation and the body weight dynamic.

1.1 Transport equation for adipocyte size evolution

Following the work in Soula et al. (2013), we first describe intake and release of lipids trough the cellular membrane, thus describing how the size of an adipose cell evolves. This will in turn allow us to build a model based on continuity equations.

Our first assumption will be the correlation between the amount of storage in an adipose cell and its radius. Cells shall be considered as spheres of a certain radius r, and the amount of lipids in the cell is denoted by x. Let us denote by $r(x)$ the radius of a cell containing x amount of lipids, by V_0 the volume of an empty cell and by V_{lipids} the molar volume of triglycerides.

We express the total volume of the cell in two different ways and we obtain the following relation:

$$V_{\text{lipids}} x + V_0 = \frac{4}{3}\pi r(x)^3,$$

which leads to:

$$r(x) = \left(\frac{3}{4\pi}(V_{\text{lipids}} x + V_0)\right)^{\frac{1}{3}}. \tag{1}$$

We also denote by L the amount of external lipids in the medium.

Henceforth, x will be considered as the size of our cell. Its variation $\frac{\mathrm{d}x}{\mathrm{d}t}$ depends on two flows: the intake of lipids by the cell from the medium and the release of lipids in the medium. As those two flows go through the membrane of the cell, they should

be surface limited. We will also consider fast diffusion of the lipids in the medium so that the amount of lipids available for each cell is the same.

The intake term is a product of three factors:

- a term for a surface limited flow $\alpha r(x)^2$, where the constant α is the rate of this flow;
- a Hill-like term with a radius cutoff ρ to describe resistance toward indefinite intake of lipids $\dfrac{\rho^n}{r(x)^n + \rho^n}$;
- a term that accounts for the available amount of lipids in the medium, in the form of a Michaelis-Menten term $\dfrac{L}{L+\kappa}$ with a saturation effect when the amount of external lipids L is large, with κ giving the order of magnitude of the threshold.

The release is a product of two terms:

- a term with a basal level of release β and a surface limited flow $\gamma r(x)^2$, where the constant γ is the release equivalent of the constant α;
- a Michaelis-Menten term for the available amount of lipids in the cell $\dfrac{x}{x+\chi}$, where χ is the equivalent of κ for the release.

The variation $\dfrac{\mathrm{d}x}{\mathrm{d}t}$ can therefore be expressed as the difference between intake and release as:

$$\frac{\mathrm{d}x}{\mathrm{d}t} = \underbrace{\alpha r(x)^2 \frac{\rho^n}{r(x)^n + \rho^n} \frac{L}{L+\kappa}}_{\text{intake}} - \underbrace{(\beta + \gamma r(x)^2) \frac{x}{x+\chi}}_{\text{release}}. \tag{2}$$

We can now build a transport equation for the distribution $f(t,x)$ of adipose cells by amount of lipids $x \geq 0$ at time t. According to Eq. (2), the transport velocity will be given by:

$$v(x, L) = a(x) \frac{L}{L+\kappa} - b(x), \tag{3}$$

where

$$a(x) = \alpha r(x)^2 \frac{\rho^n}{r(x)^n + \rho^n} \tag{4}$$

and

$$b(x) = (\beta + \gamma r(x)^2) \frac{x}{x+\chi}. \tag{5}$$

Consequently, the function f satisfies the following transport equation:

$$\partial_t f(t,x) + \partial_x (v(x, L) f(t,x)) = 0, \qquad x \geq 0, \qquad t > 0. \tag{6}$$

We now need to describe the behaviour of the available amount of lipids in the medium L. As per our assumption, the total quantity of lipids in our system, denoted by λ, should be constant. There are two types of lipids in the system: the ones contained in the cells, and the lipids in the medium and we therefore have the following equality:

$$L(t) + \int_{\mathbb{R}_+} x f(t,x) \mathrm{d}x = \lambda. \tag{7}$$

Another hypothesis is that the number of adipocytes does not change in time. Thus, in regards to boundary conditions, we want to preserve the total population number and therefore we impose that:

$$\int_{\mathbb{R}_+} f(t,x) \mathrm{d}x = \int_{\mathbb{R}_+} f^0(x) \mathrm{d}x = m \text{ for all } t > 0. \tag{8}$$

This leads for Eq. (6) to boundary condition

$$(v(x, L(t)) f(t,x))\big|_{x=0} = 0, \quad \text{for all } t > 0. \tag{9}$$

Notice that by Eqs. (4)–(5), we have $b(0) = 0$ and $a(0) > 0$. Hence, the boundary conditions (9) is equivalent to the Dirichlet boundary condition:

$$f(t,x)\big|_{x=0} = 0 \text{ for all } t > 0. \tag{10}$$

To sum up, the transport model for adipose cells with initial conditions (f^0, L^0), that will be called first-order Lifshitz–Slyozov model in the following, reads as:

$$\begin{cases} \partial_t f(t,x) + \partial_x (v(x, L(t)) f(t,x)) = 0, & \text{(11a)} \\ L(t) + \displaystyle\int_{\mathbb{R}_+} x f(t,x) \mathrm{d}x = \lambda, & \text{(11b)} \\ (v(x, L(t)) f(t,x))\big|_{x=0} = 0, & \text{(11c)} \\ f(0,x) = f^0(x) \text{ and } L(0) = L^0. & \text{(11d)} \end{cases}$$

Regarding the value of the parameters of the model, a biological estimation of both β the basal release rate and γ the surface release rate were made from biological experiments in Soula et al. (2015). The value for other parameters are estimated in Giacobbi et al. (2023) thanks to experimental data.

1.2 New models for adipose tissue dynamics

In this subsection, we present the various models under consideration in this article. Starting from the description of lipogenesis and lipolysis as done in Eqs. (4) and (5) following (Soula et al. 2013), we build size-structured PDE model following the

framework of Becker–Döring system (Becker and Döring 1935) and Lifshitz–Slyozov equations (Lifshitz and Slyozov 1961) initially derived for polymerization.

The aim of this model is to reproduce the adipocyte size distributions observed experimentally and their bimodal structure. However, the transport equation (6) possesses asymptotic solutions as a linear combination of Dirac masses centered on the zeros of the asymptotic speed. This was proved in Collet et al. (2002); Calvo et al. (2018) for simpler choices of the rates a and b and in the case of convergence toward a single Dirac mass, but these results are currently not applicable to our model. Solutions with growing and unbounded support, with self-similar long-time behavior, have been detailed for the Lifshitz–Slyozov and Lifshitz–Slyozov–Wagner models, notably in Niethammer and Pego (1999). However this situation has been described for coefficients such that $\lim_{x\to\infty} \frac{b(x)}{a(x)} = 0$ (the most common choice being $a(x) = x^{1/3}$ and $b(x) = 1$, shown to be physically relevant Niethammer 2004). This choice together with monotonicity ensures a crucial assumption on the velocity (Calvo et al. 2021), which is the existence of some critical size x_{crit} (t) such that for all $x \leq x_{crit}(t)$ the velocity $v(x, L(t))$ is negative, and positive for all $x \geq x_{crit}(t)$. For the case of adipose cell modeling, the choice of a and b is rather complex and in most cases the velocity changes sign multiple times, but from numerical simulations, see Figs. 10, 11 and 12, we believe the asymptotic solution to be a linear combination of Dirac masses. Actually, due to the boundedness of a and strict monotonicity of b, starting from a compactly supported solution, it is for instance easy to show that the support of the solution stays in a compact set, uniformly in time (see lemma 6.1 in Annex). Additionnally from numerical simulations, see Fig. 10, and from the fact that we are in the sub-critical case, we do not believe such behaviours to be likely to happen here. Moreover, due to the boundedness of a, starting from a compactly supported solution, it is for instance easy to show that the support of the solution stays in a compact, uniformly in time.

Hence even if the stationary solutions of system (11) are able to recover the position of the two peaks, we are interested in a model that is able to recover the whole range of possible sizes. A natural extension is therefore to include a diffusion term to the transport equation (11) which is expected to smooth the stationary solutions. We can either add a diffusion term with a constant rate with no real biological meaning, or we can compute a time and space dependent diffusion term coming from the discrete nature behind the Lifshitz–Slyozov formalism (Hariz and Collet 1999; Vasseur et al. 2002). For that purpose, we come back to a Becker–Döring system of ODEs giving the evolution with respect to time of the number of adipocytes with discrete sizes and from this, we derive a second order Lifshitz–Slyozov equation with a diffusion term.

Note that our final goal, which is out of the scope of the present article, is to perform parameter estimation thanks to experimental data. For that purpose, asymptotic solutions to Lifshitz–Slyozov equation with diffusion, which are smooth functions, are more adapted than the discontinuous asymptotic solutions to Lifshitz–Slyozov equation or than the discrete solutions to the Becker–Döring equation.

Therefore, in the following, we will consider three different models for the size distribution of an adipocyte population, namely

- the ODE system (14) with discrete sizes, a variant of the Becker–Döring model.

- the previously published transport equation (11), also called first order Lifshitz–Slyozov equation,
- the transport-diffusion equation (18), the second order Lifshitz–Slyozov equation.

In all three models, the lipogenesis and lipolysis rate will be given by Eq. (4) and (5), respectively.

Note that we impose in all three models two conservation laws: (i) the conservation of the total amount of lipids and (ii) the conservation of the total number of adipocytes. Therefore, all these models have a constant population number and are coupled with a lipid conservation equation which ensures that the sum of the lipids in the external medium and the lipids inside the cells is constant.

1.2.1 A brief insight into the Becker–Döring equations

Becker–Döring equations have been introduced in Becker and Döring (1935) to model polymers undergoing aggregation and fragmentation. The Lifshitz–Slyozov model was introduced in Lifshitz and Slyozov (1961) and first used for nucleation in supersaturated solid solutions and polymerisation processes. A rigourous treatment of the mathematical properties of the Becker–Döring equations was given by Ball et al. (1986). The relation between Becker–Döring equations and Lifshitz–Slyozov model goes back to Penrose et al. (1978). For a detailed review of both models, see Hingant and Yvinec (2017) and references therein.

Let us explain briefly the idea of these models for polymers. We denote by c_i, the amount of polymers containing i monomers for $i \in \mathbb{N}^*$ and hence c_1 stands for the amount of monomers. A polymer of size i denoted p_i can gain one monomer and grow to p_{i+1} with rate a_i or lose one monomer and shrink to p_{i-1} with rate b_i. We may write as a system of ODEs for the time evolution of the number of polymers c_i, one for each size i. Furthermore, the total amount of monomers, i.e free monomers and monomers within polymers, is assumed constant, which leads to a conservation equation. Stationary solutions of the Becker–Döring equations can be easily computed, and long time behaviour has been characterized by Ball et al. (1986).

1.2.2 A brief insight into the Lifshitz–Slyozov equations

Another possibility for the modeling of polymerisation-fragmentation processes is to describe continuously the size of polymers through a variable $x \in \mathbb{R}$. The distribution of polymers of size x at time t is therefore denoted by $f(t, x)$ and the quantity of monomers at time t is denoted by $L(t)$. The distribution is classically transported as in Eq. (6) with speed $v(x, L) = a(x)L(t) - b(x)$ where $a(x)$ is the rate of polymerisation for size x and $b(x)$ is the rate of depolymerisation for size x. As previously, the total amount of monomers is conserved. Depending on the sign of $a(0)L(t) - b(0)$, boundary conditions should be provided for the system, see Deschamps et al. (2017) for example.

After an adapted rescaling, it has been shown in various papers (Conlon and Schlichting 2019; Deschamps et al. 2017; Laurençot and Mischler 2002; Niethammer 2004; Schlichting 2019; Vasseur et al. 2002) that the solutions to Becker–Döring system tend to the solutions to Lifshitz–Slyozov model. Formally, the limit up to

second order can be considered and gives rise to an advection–diffusion equation as computed in Hariz and Collet (1999); Vasseur et al. (2002). Existence of solutions is widely known for both models, see the seminal paper (Ball et al. 1986) for the Becker–Döring model and (Calvo et al. 2021; Collet and Goudon 2000) for the Lifshitz–Slyozov model..

Remark that Becker–Döring and Lifshitz–Slyozov equations have already been used in various contexts, for example modeling of biological phenomena, such as prions (Doumic et al. 2009; Laurençot and Walker 2007; Simonett and Walker 2006; Prigent et al. 2012; Greer et al. 2006) or modeling in oceanography, see (Wurl et al. 2011; Jackson and Burd 1998).

1.2.3 A Becker–Döring model for adipose cells

Now, let us explain how we adapt this formalism to derive new models for adipocyte size dynamics. The purpose of this construction is to investigate the classical convergence theorems from Becker–Döring to Lifshitz–Slyozov and deduce the form of a diffusion term to add in our model.

We mention the main differences with the classical Becker–Döring and Lifshitz–Slyozov systems for polymerisation. First, velocity (2), arising from biological considerations, possesses three zeros for a well-chosen range of parameters which leads to bimodal asymptotic distributions, whereas classical choices for a and b are constant or power laws of x, which yields the existence of a single positive root. See also Calvez et al. (2010) for a polymerisation-fragmentation model without diffusion giving rise to bimodal asymptotics. Second, in our model, external lipids L cannot be assimilated to monomers c_1 and the conservation law (7) is therefore not the same as in the usual polymerisation models. Moreover, the saturation term $\frac{L}{L+\kappa}$ is not common in polymerisation modeling. Finally, our model conserves the total population number due to the boundary condition (11c), which adds an additional conservation law compared to the classical Becker–Döring model.

We shall now consider that an adipose cell is a bundle of smaller vesicles of typical size Λ. Hence the size of a cell can be defined by the number of vesicles it contains. We denote by c_i the number of cells of size i and by l the number of vesicles in the medium. A cell will aggregate a new vesicle with speed $a_i M(l)$,where $M(l) = \frac{l\Lambda}{l\Lambda+\kappa}$ following Eq. (2), and loose a vesicle at speed b_i, following this reaction:

$$\Lambda + i\Lambda \underset{b_{i+1}}{\overset{a_i M(l)}{\rightleftharpoons}} (i+1)\Lambda.$$

We define $c = (c_i)_{i\geq 0}$ and $J_i(c,l)$ the flow of the previous reaction given by:

$$J_i(c,l) = a_i M(l) c_i - b_{i+1} c_{i+1}, i \geq 0, \tag{12}$$

where a_i (resp. b_i) is a discrete counterpart of the continuous function a defined at Eq. (4) (resp. b defined at Eq. (5)).

Therefore, the Becker–Döring system may be written as:

$$\begin{cases} \dfrac{dc_i}{dt} = J_{i-1}(c,l) - J_i(c,l), \ \forall i \geq 1, & \text{(13a)} \\ \dfrac{dc_0}{dt} = -J_0(c,l), & \text{(13b)} \\ l(t)\Lambda + \displaystyle\sum_{i=0}^{\infty} i\Lambda c_i(t) = \lambda, \ \forall t \geq 0, & \text{(13c)} \\ l(0) = l^0, \quad c_i(0) = c_i^0, \ \forall i \geq 1. & \text{(13d)} \end{cases}$$

The rescaling procedure we use is akin to the one in Deschamps et al. (2017); Vasseur et al. (2002). We introduce the following scaling constants:

- $\bar{A}$ rescaling value of $(a_i)_{i\geq 0}$,
- $\bar{B}$ rescaling value of $(b_i)_{i\geq 1}$,
- $\bar{C}$ rescaling value of $(c_i)_{i\geq 0}$,
- $\bar{T}$ rescaling value of the time scale,

We previously denoted by Λ the typical size of a vesicle. Hence it plays the role of a rescaling value and should be treated as so.

Now, we introduce the rescaled variables:

$$\begin{aligned} \bar{a_i} &= \frac{a_i}{\bar{A}}, \ \forall i \geq 0, \\ \bar{b_i} &= \frac{b_i}{\bar{B}}, \ \forall i \geq 0, \\ \bar{t} &= \frac{t}{\bar{T}}, \\ \bar{c_i}(\bar{t}) &= \frac{c_i(\bar{t}\bar{T})}{\bar{C}}, \ \forall i \geq 0, \\ \bar{L}(\bar{t}) &= l(\bar{t}\bar{T})\Lambda. \end{aligned}$$

The quantity $\bar{L}$ therefore describes the total amount of lipids in the medium instead of the number of lipid vesicles.

We compute from equation (13) the derivative of $\bar{c_i}$ for $i \geq 1$:

$$\begin{aligned} \frac{d\bar{c_i}}{dt}(\bar{t}) &= \frac{\bar{T}}{\bar{C}}\frac{dc_i}{dt}(\bar{t}\bar{T}) \\ &= \frac{\bar{T}}{\bar{C}}\Big(a_{i-1}\frac{l(\bar{t}\bar{T})\Lambda}{l(\bar{t}\bar{T})\Lambda+\kappa}c_{i-1}(\bar{t}\bar{T}) - (a_i\frac{l(\bar{t}\bar{T})\Lambda}{l(\bar{t}\bar{T})\Lambda+\kappa} + b_i)c_i(\bar{t}\bar{T}) + b_{i+1}c_{i+1}(\bar{t}\bar{T})\Big) \\ &= \bar{A}\bar{T}\Big(\bar{a}_{i-1}\frac{\bar{L}(\bar{t})}{\bar{L}(\bar{t})+\kappa}\bar{c}_{i-1}(\bar{t}) - \bar{a}_i\frac{\bar{L}(\bar{t})}{\bar{L}(\bar{t})+\kappa}\bar{c}_i(\bar{t})\Big) - \bar{B}\bar{T}\Big(\bar{b}_i\bar{c}_i(\bar{t}) - \bar{b}_{i+1}\bar{c}_{i+1}(\bar{t})\Big). \end{aligned}$$

The derivative of $\bar{c_0}$ writes as:

$$\frac{d\bar{c}_0}{dt}(\bar{t}) = -\bar{A}\bar{T}\bar{a}_0\frac{\bar{L}(\bar{t})}{\bar{L}(\bar{t})+\kappa}\bar{c}_0(\bar{t}) + \bar{B}\bar{T}\bar{b}_1\bar{c}_1(\bar{t})$$

and the conservation equation for lipids as:

$$\bar{L}(\bar{t}) + \bar{C}\Lambda \sum_{i\geq 1} i\bar{c}_i(\bar{t}) = \lambda.$$

We now relate all the rescaling constants to a single variable $\varepsilon > 0$, such that:

$$\bar{A}\bar{T} = \bar{B}\bar{T} = \frac{1}{\varepsilon}, \bar{C}\Lambda = \varepsilon^2 \text{ and } \delta = \varepsilon.$$

At last, we drop the bar above the variables and replace it with ε as superscript to show the dependency of the solution on ε.

Remark Depending on the process we are trying to model, the interpretation of the rescaling may vary. Some rescaling procedures intend to capture the large time asymptotic of the Becker–Döring model (Niethammer 2004; Conlon and Schlichting 2019) while others are more in the spirit of hydrodynamic limits (Laurençot and Mischler 2002; Vasseur et al. 2002), using assumptions on initial conditions and coefficients. For adipose cells we fall into the latter case: this rescaling can be seen as if the rate of reactions is of order $\frac{1}{\varepsilon}$, but each reaction size is of order ε and the size of the individual vesicles is also of order ε.

We finally get the following ODE system:

$$\begin{cases} \dfrac{dc_i^\varepsilon}{\mathrm{d}t} = \dfrac{1}{\varepsilon}(J_{i-1}^\varepsilon(c^\varepsilon, L^\varepsilon) - J_i^\varepsilon(c^\varepsilon, L^\varepsilon)), \ \forall i \geq 1, & \text{(14a)} \\ \dfrac{dc_0^\varepsilon}{\mathrm{d}t} = -\dfrac{1}{\varepsilon}J_0^\varepsilon(c^\varepsilon, L^\varepsilon), & \text{(14b)} \\ L^\varepsilon(t) + \displaystyle\sum_{i=0}^{\infty} i\varepsilon^2 c_i^\varepsilon(t) = \lambda, \ \forall t \geq 0, & \text{(14c)} \\ L^\varepsilon(0) = L^{\varepsilon,0}, \quad c_i^\varepsilon(0) = c_i^{\varepsilon,0}, \ \forall i \geq 1, \ \forall i \geq 0, & \text{(14d)} \end{cases}$$

which is similar to Becker–Döring equations except for the definition of the flux J_i^ε (saturating fluxes of monomers)

$$J_i^\varepsilon(c^\varepsilon, L^\varepsilon) = a_i^\varepsilon \frac{L^\varepsilon}{L^\varepsilon + \kappa} c_i^\varepsilon - b_{i+1}^\varepsilon c_{i+1}^\varepsilon$$

and the minimal size is 0 and not 1. Proper assumptions on the discrete rates are given at the beginning of Sect. 2. Observe also that there is no 'boundary' flux, thus the quantity

$$m = \varepsilon \sum_{i\geq 0} c_i^\varepsilon(t) \text{ is constant in time.} \quad (15)$$

This is the discrete analogue to the previous conservation (8) of the zeroth order moment of f.

A solution to the previous system exists according to Theorem 2.1 recalled in Sec. 2. Now let us define the following step functions depending on both time and space:

$$f^\varepsilon(t,x) = \sum_{i\geq 0} \mathbb{1}_{\Gamma_i^\varepsilon}(x) c_i^\varepsilon(t),$$

where $\Gamma_i^\varepsilon = [(i-\frac{1}{2})\varepsilon, (i+\frac{1}{2})\varepsilon[$, and $(c_i^\varepsilon)_{i\geq 0}$ is a solution to (14).

Convergence of function f^ε when $\varepsilon \to 0$ towards a solution f of the Lifshitz–Slyozov equation (11) is a classical result, see Theorem 2.3 recalled in Sec. 2. In the present work, we prove that a similar convergence result hold in a stronger topology, and with a control of the speed of convergence, of order at least ε.

To that, we introduce the tail distributions:

$$F(t,x) = \int_x^\infty f(t,y)\mathrm{d}y, \qquad F^\varepsilon(t,x) = \int_x^\infty f^\varepsilon(t,y)\mathrm{d}y.$$

The main analytical result of this article is the following theorem, whose more rigorous statement will be specified later in Theorem 3.1:

Theorem 1.1 (Convergence of tails of distributions) *Let $T > 0$. Suppose that there exists some constant $C_{\text{init}} > 0$ such that for all $\varepsilon > 0$, $\int_{\mathbb{R}_+} |F^\varepsilon(0,x) - F(0,x)|\mathrm{d}x \leq \varepsilon C_{\text{init}}$. Also assume that hypotheses (H1)–(H9) hold true. Then there exists some constants $C(T) > 0$ (independent of ε) and ε^* (independent of T) and such that for all $0 < \varepsilon \leq \varepsilon^*$ and for all $t \in (0,T]$:*

$$|L^\varepsilon(t) - L(t)| + \int_{\mathbb{R}_+} |F^\varepsilon(t,x) - F(t,x)|\mathrm{d}x \leq \varepsilon C(T).$$

This result provides a new approach for looking into convergence from Becker–Döring to Lifshitz–Slyozov. Contrary to more classical results where convergence towards a weak solution is achieved using Ascoli-Arzela's Theorem, this theorem yields convergence towards mild solutions and gives a bound of order ε on the speed of this convergence.

Stationary solutions of the Becker–Döring equations have an explicit formulation, see Ball et al. (1986). However since the model we introduced has no biological relevance, we are not interested in studying them. Moreover we are ultimately interested in doing parameter estimation on biological data and a continuous model is more suited to the methods we want to use. Also, establishing a theoretical connection between the stationary states of the Becker–Döring and Lifshitz–Slyozov equations is not a trivial matter. In Hariz and Collet (1999), the authors introduced a diffusive term to the Lifshitz–Slyozov model, whith the intend that this modified Lifshitz–Slyozov model will have stationary states which are more easily linked to the stationary states of the

Becker–Döring model. There are able to establish a connection when the rates are constants and where λ is close to the critical value $\lim_{x\to\infty} \frac{b(x)}{a(x)}$. We shall see in the next section a slightly different version of this diffusive Lifshitz–Slyozov model which we call the second-order Lifshitz–Slyozov model, the difference being in the boundary condition. Nonetheless, for a general choice of rates a and b, we are unaware of results establishing a theoretical connection between the stationary states of both models.

1.2.4 A second order Lifshitz–Slyozov model

Another goal in this article is to derive a new model with a diffusive term from Becker–Döring system (14). One can see this diffusive term as a second order term emerging from the convergence theorem 3.1. There are various ways to yield this term, see for example (Vasseur et al. 2002; Schlichting 2019; Deschamps et al. 2017). The derivation of the diffusive term will be detailed in Sect. 4, but we present the model here for the sake of completeness.

The so-called second order Lifshitz–Slyozov model therefore takes the form of a transport-diffusion equation, with a diffusive term which depends both on x and $L(t)$, i.e.:

$$\partial_t g + \partial_x(vg) = \frac{\varepsilon}{2}\partial_x^2(dg), \qquad \forall x \geq 0,$$

where

$$d : (x, L) \in \mathbb{R}_+ \times \mathbb{R}_+ \to d(x, L) = a(x)\frac{L}{L+\kappa} + b(x). \tag{16}$$

We need to complement this PDE with adapted boundary conditions. Since we want the conservation of the zeroth order moment denoted by $\int_{\mathbb{R}_+} g(t, x)\mathrm{d}x = m$, we need to impose the following null-flux boundary condition:

$$(-vg + \frac{\varepsilon}{2}\partial_x(dg))\Big|_{x=0} = 0. \tag{17}$$

Therefore, we consider the following system, which consists of the previous PDE and boundary conditions, complemented by previous constraint (7) and initial conditions for g and L:

$$\begin{cases} \partial_t g + \partial_x(vg) = \frac{\varepsilon}{2}\partial_x^2(dg), & \text{(18a)} \\ L(t) + \int_{\mathbb{R}_+} xg(t, x)\mathrm{d}x = \lambda, & \text{(18b)} \\ \Big(- vg + \frac{\varepsilon}{2}\partial_x(dg)\Big)\Big|_{x=0} = 0, & \text{(18c)} \\ g(0, x) = g^0(x) \text{ and } L(0) = L^0. & \text{(18d)} \end{cases}$$

We provide interesting numerical evidence of stationary solutions of the advection–diffusion model (18) following a bimodal distribution. The numerical simulations are performed using a well-balanced scheme developped in Goudon and Monasse (2020). We also demonstrate that to observe a bimodal asymptotics, parameters should be taken into an adapted parameter range.

1.3 Outline of the article

In Sect. 2, we will give some preliminary results on the existence of solutions to systems (14) and (11). In Sect. 3, we will show the convergence theorem thanks to the tail of distributions technique. Then, in Sect. 4, we derive formally the second-order Lifshitz–Slyozov model, that is to say system (18) and we give the expression for its stationary solutions. In Sect. 5, we display some numerical results and we show that bimodality of the stationary solution can be observed in well-chosen parameter range. Finally, we discuss our results in Sect. 6.

2 Preliminary results

In this section, we give the main already-known results of existence of solutions to systems (14) and (11) and convergence of solutions to system (14) towards (11). Proofs have been easily adapted to our framework.

2.1 Existence results on Becker–Döring system

We consider first the Becker–Döring system (14) for fixed ε. From the modeling we introduced for adipose cells, we have an explicit expression for the functions a and b, from which we deduce consistent discrete approximations, in the spirit of numerical analysis (see for instance Laurençot and Mischler 2002). In turn, we will introduce assumption (H4) that relates a_i^ε to a and b_i^ε to b when we describe the convergence result. However when studying the existence of solutions to the Becker–Döring system, we can take weaker assumptions on the rates a_i^ε and b_i^ε. Nonetheless assumptions (H1)–(H4) imply both assumptions (H'1) and (H'2).

We assume that there exist some strictly positive constants A, B, C_a, C_b, K_a, K_b and δ, all independent of ε, such that for all $i \geq 0$:

$$a_i^\varepsilon \leq C_a \text{ and } b_i^\varepsilon \leq C_b i\varepsilon, \tag{H'1}$$

$$|a_i^\varepsilon - a_{i+1}^\varepsilon| \leq K_a\varepsilon \text{ and } |b_i^\varepsilon - b_{i+1}^\varepsilon| \leq K_b\varepsilon. \tag{H'2}$$

The classical result of existence in Ball et al. (1986) assumes $a_i, b_i = O(i)$, with typical coefficients being of the form $a_i = i^\mu$, $b_i = i^\nu$, $0 \leq \nu, \mu < 1$ as well as additional assumptions on the initial conditions. These assumptions were relaxed in Laurençot and Mischler (2002), by considering 'smooth' coefficients in the sense of

assumption (H'2). Assumption (H'1) ensures that for large i we fall into the case $a_i, b_i = O(i)$. Note that our model with assumptions (H'1) and (H'2) falls into the classical choices for the rates a_i and b_i because we already know the target rate functions a and b, which are smooth, bounded for a, and sub-linear for b.

We define the state space for Eq. (14) by

$$X := \left\{ x = (x_i)_{i\geq 0} \in \mathbb{R}_+^{\mathbb{N}} : \sum_{i=0}^{+\infty} i x_i < \infty \right\},$$

endorsed with the norm $\|x\|_X = \sum_{i=0}^{+\infty} i|x_i|$. We denote $x \geq 0$ if $x_i \geq 0$ for all $i \geq 0$, and $X^+ := \{x \in X : x \geq 0\}$. We give the following definition of solution to Eq. (14):

Definition 2.1 Let $T > 0$ and $\varepsilon > 0$. A solution $(c^\varepsilon, L^\varepsilon)$ of (14) in $[0, T)$ is a pair of a function $L^\varepsilon : [0, T) \to \mathbb{R}$ and a sequence of functions $c^\varepsilon = (c_i^\varepsilon)_{i\geq 0}$, $c_i^\varepsilon : [0, T) \to X$ such that:

(i) For all $t \in [0, T)$, $L^\varepsilon(t) \geq 0$ and $c^\varepsilon(t) \in X^+$,
(ii) For all $i \geq 1$, $c_i^\varepsilon : [0, T) \to \mathbb{R}$ is continuous and $\sup_{t\in[0,T)} \|c^\varepsilon(t)\|_X < +\infty$,
(iii) $L^\varepsilon : [0, T) \to \mathbb{R}$ is continuous and $\sup_{t\in[0,T[} |L^\varepsilon(t)| < +\infty$,
(iv) For all $t \in [0, T)$, $\int_0^t \sum_{i=0}^{+\infty} a_i^\varepsilon c_i^\varepsilon(s)\mathrm{d}s < \infty$ and $\int_0^t \sum_{i=0}^{+\infty} b_i^\varepsilon c_i^\varepsilon(s)\mathrm{d}s < \infty$,
(v) For all $t \in [0, T)$, for all $i \geq 1$:

$$c_i^\varepsilon(t) = c_i^{\varepsilon,0} + \frac{1}{\varepsilon}\int_0^t [J_{i-1}^\varepsilon(c^\varepsilon(s), L^\varepsilon(s)) - J_i^\varepsilon(c^\varepsilon(s), L^\varepsilon(s))]\mathrm{d}s,$$

$$c_0^\varepsilon(t) = c_0^{\varepsilon,0} - \frac{1}{\varepsilon}\int_0^t J_0^\varepsilon(c^\varepsilon(s), L^\varepsilon(s))\mathrm{d}s,$$

$$L^\varepsilon(t) = L^{\varepsilon,0} - \varepsilon\int_0^t \sum_{i=0}^{+\infty} J_i^\varepsilon(c^\varepsilon(s), L^\varepsilon(s))\mathrm{d}s$$

Well-posedness of solutions to (14) as defined at Def.2.1 can be shown by finite dimensional approximation, using the method developped in Ball et al. (1986):

Theorem 2.1 *Let $T > 0$ and $\varepsilon > 0$. Let $L^{\varepsilon,0} \in \mathbb{R}_+$ et $c^{\varepsilon,0} \in X^+$ such that $L^{\varepsilon,0} + \sum_{i=0}^{+\infty} i\varepsilon^2 c_i^{\varepsilon,0} = \lambda < \infty$. Assume that (H'1), (H'2) hold true. Then there exists a unique solution $(c^\varepsilon, L^\varepsilon)$ to Becker–Döring system (14) in the sense of Def. 2.1 which satisfies initial conditions $c^\varepsilon(0) = c^{\varepsilon,0}$ and $L^\varepsilon(0) = L^{\varepsilon,0}$.*

The uniqueness and conservation properties of the solution are obtained using the following proposition that will be needed later on, see Sec. 4. In particular, the following proposition states that any solution of the Becker–Döring system (14) preserves the first two moments for all times, and provides the starting point to compute any admissible moments for the solution of the Becker–Döring system. In Ball et al. (1986), we can find the following Theorem 2.5 that we reproduce here for the reader's convenience:

Proposition 2.1 *Let $(\phi_i)_{i\geq 0}$ be a given sequence. Let $(c^\varepsilon, L^\varepsilon)$ be the solution of (14) on $[0, T)$, $0 < T \leq +\infty$.*

Assume that for all $0 \leq t_1 < t_2 < T$, $\int_{t_1}^{t_2} \sum_{i=0}^{\infty} |\phi_{i+1} - \phi_i| a_i^\varepsilon c_i^\varepsilon(t)\mathrm{d}t < \infty$ and that either of the following holds:

(a) $\phi_i = \mathcal{O}(i)$ *and* $\int_{t_1}^{t_2} \sum_{i=0}^{\infty} |\phi_{i+1} - \phi_i| b_{i+1}^{\varepsilon} c_{i+1}^{\varepsilon}(t)\mathrm{d}t < \infty$ *or*

(b) $\sum_{i=0}^{\infty} \phi_i c_i^{\varepsilon}(t_k) < \infty$, *for* $k = 1, 2$ *and* $\phi_{i+1} \geq \phi_i \geq 0$ *for* i *large enough.*

Then:

$$\sum_{i=0}^{\infty} \phi_i c_i^{\varepsilon}(t_2) - \sum_{i=0}^{\infty} \phi_i c_i^{\varepsilon}(t_1) + \int_{t_1}^{t_2} \sum_{i=0}^{\infty} \frac{\phi_{i+1} - \phi_i}{\varepsilon} b_{i+1}^{\varepsilon} c_{i+1}^{\varepsilon}(t)\mathrm{d}t = \int_{t_1}^{t_2} \sum_{i=0}^{\infty} \frac{\phi_{i+1} - \phi_i}{\varepsilon} a_i^{\varepsilon} \frac{L^{\varepsilon}(t)}{L^{\varepsilon}(t) + \kappa} c_i^{\varepsilon}(t)\mathrm{d}t.$$

2.2 Lifshitz–Slyozov system and classical convergence result

Even though we have precise forms for the intake and release functions, for the sake of generality we make the following assumptions on functions a and b occurring in Eq. (46):

$$a, b \in C^1(\mathbb{R}_+, \mathbb{R}_+), \tag{H1}$$

$$a(0) > 0 \text{ and } \sup_{x \in \mathbb{R}_+} |a(x)| = C_a, \tag{H2a}$$

$$|b(x)| \leq C_b x \text{ for all } x \in \mathbb{R}_+ \text{ and } \lim_{R \to \infty} \sup_{x \geq R} \frac{b(x)}{x} = 0, \tag{H2b}$$

$$\sup_{x \in \mathbb{R}_+} |a'(x)| = K_a \text{ and } \sup_{x \in \mathbb{R}_+} |b'(x)| = K_b, \tag{H3}$$

with $C_a, C_b, K_a, K_b > 0$. We first define measured-valued solutions to the Lifshitz–Slyozov system (11), following (Collet and Goudon 2000)

Definition 2.2 Given an initial condition $(f^0, L^0) \in C^0(\mathbb{R}_+) \cap L^1(\mathbb{R}_+, (1+x)\mathrm{d}x) \times \mathbb{R}_+$, a measured-valued solution to system (11) is composed of two functions $f \in C(0, T; \mathcal{M}^1(0, \infty) - weak - *)$ and $L \in C(0, T)$ such that for all $0 < t < T$ and for all $\varphi \in C^1([0, T] \times \mathbb{R}_+)$ the following relations hold:

$$\int_0^T \int_{\mathbb{R}_+} (\partial_t \varphi(t, x) + v(x, L(t)) \partial_x \varphi(t, x)) f(t, x)\mathrm{d}x + \int_{\mathbb{R}_+} \varphi(0, x) f^0(x)\mathrm{d}x = 0,$$
$$L(t) + \int_{\mathbb{R}_+} x f(t, x)\mathrm{d}x = \lambda.$$

Now, let us state the convergence of solutions to Becker–Döring system towards solutions to Lifshitz–Slyozov system. In order to compare solutions to Becker–Döring system to solutions to Lifshitz–Slyozov system, we need to define the following piecewise constant functions. Let $\Gamma_i^{\varepsilon} = [(i - \frac{1}{2})\varepsilon, (i + \frac{1}{2})\varepsilon)$ and c_i^{ε} be solutions to (14),

then we define

$$\begin{cases} f^\varepsilon(t,x) = \sum_{i\geq 0} \mathbb{1}_{\Gamma_i^\varepsilon}(x) c_i^\varepsilon(t)\,, & \text{(19a)} \\ a^\varepsilon(x) = \sum_{i\geq 0} \mathbb{1}_{\Gamma_i^\varepsilon}(x) a_i^\varepsilon\,, & \text{(19b)} \\ b^\varepsilon(x) = \sum_{i\geq 1} \mathbb{1}_{\Gamma_i^\varepsilon}(x) b_i^\varepsilon\,, & \text{(19c)} \end{cases}$$

where we assume that:

$$a_i^\varepsilon = a(i\varepsilon) \text{ and } b_i^\varepsilon = b(i\varepsilon), \text{ for all } i \geq 0 \text{ and } \varepsilon > 0. \tag{H4}$$

Given our definitions in Eq. (19), from Proposition 2.1 and with $\phi_i = \int_{\Gamma_i^\varepsilon} \phi(x)\mathrm{d}x$, we deduce the following proposition, that is the starting point to study the convergence of the solution of the Becker–Döring system (14) towards solution of the Lifshitz–Slyozov equation (11).

Proposition 2.2 *Let $\phi \in L^\infty(\mathbb{R}_+)$. Then for every $t \geq 0$, we have the following equality:*

$$\begin{aligned} &\int_0^\infty \phi(x)(f^\varepsilon(t,x) - f^\varepsilon(0,x))\mathrm{d}x \\ &= \int_0^t \int_0^\infty (\Delta_\varepsilon \phi(x) a^\varepsilon(x) \frac{L^\varepsilon(t)}{L^\varepsilon(t)+\kappa} - \Delta_{-\varepsilon}\phi(x) b^\varepsilon(x)) f^\varepsilon(t,x)\mathrm{d}x\mathrm{d}t, \end{aligned}$$

where

$$\Delta_\varepsilon \phi(x) = \frac{\phi(x+\varepsilon) - \phi(x)}{\varepsilon}. \tag{20}$$

Finally, we obtain the following convergence theorem from the Becker–Döring equations to the Lifshitz–Slyozov equations, as in Vasseur et al. (2002):

Theorem 2.2 *Consider an initial condition $(L^{\varepsilon,0}, (c_i^{\varepsilon,0})_{i\geq 0})$ and the corresponding solution $(L^\varepsilon, (c_i^\varepsilon)_{i\geq 0})$ in the sense of Definition 2.1. We assume that there exists a constant $K > 0$ and $0 < s \leq 1$ both independent of ε such that:*

- $L^{\varepsilon,0} + \varepsilon^2 \sum_{i\geq 0} i c_i^{\varepsilon,0} = \lambda$,
- $\varepsilon \sum_{i\geq 0} c_i^{\varepsilon,0} < K$,
- $\varepsilon \sum_{i\geq 0} (i\varepsilon)^{1+s} c_i^{\varepsilon,0} < K$.

We also assume hypotheses (H1)–(H4) to hold. Then there exists a sequence ε_n and a solution (f, L) to (11) in the sense of Definition 2.2 such that:

$$\begin{cases} f^{\varepsilon_n} \to f\,, \quad x f^{\varepsilon_n} \to x f \text{ in } C^0([0,+\infty[; \mathcal{M}^1(0,+\infty) - weak - *), \\ L^{\varepsilon_n} \to L \text{ uniformly in } C^0([0,T]). \end{cases}$$

Now, let us consider the existence of mild solutions to (11). For that purpose, we first define the characteristic curves.

Assume $L \in C^0(\mathbb{R}_+)$ to be given. The characteristic curves associated to (11) are solutions to:

$$\begin{cases} \partial_s X(s;t,x) = v(X(s;t,x), L(s)), \\ X(t;t,x) = x. \end{cases}$$

Since v is C^1 in both x and L, the characteristics are uniquely defined and form an ordered family. We denote $I_{t,x}$ their maximal time interval and by $X_c(t) = X(t;0,0)$ the characteristic curve that is equal to 0 at time 0. Then, a mild solution to system (11) is given by the following definition:

Definition 2.3 Given a smooth initial condition f^0 and $L \in C^0(\mathbb{R}_+)$, a mild solution of

$$\begin{cases} \partial_t f + \partial_x (v(x, L(t)) f) = 0, \\ (v(x, L(t)) f(t,x))\big|_{x=0} = 0, \\ f(0,x) = f^0(x), \end{cases}$$

is given by:

$$f(t,x) = f^0(X(0;t,x)) \exp\left(- \int_0^t \partial_x v(X(s;t,x), L(s)) ds \right) \mathbb{1}_{(X_c(t),\infty)}(x).$$

A pair (f, L) is said to be a solution of (11) if f is a mild solution associated to L and $L : \mathbb{R}_+ \to \mathbb{R}_+$ solves $L(t) + \int_{\mathbb{R}_+} x f(t,x) \mathrm{d}x = \lambda$ for all $t \geq 0$.

Remark Since we impose null-flux boundary conditions on this system: $v(x, L(t)) f(t, x)|_{x=0} = 0$, there is no term involving "incoming characteristics" $\mathbb{1}_{(0,X_c(t))}(x)$.

We follow the proofs in Collet and Goudon (2000) and Calvo et al. (2021) and we obtain in a straightforward way the expected existence and uniqueness result:

Theorem 2.3 *Given an initial condition* $(f^0, L^0) \in C^0(\mathbb{R}_+) \cap L^1(\mathbb{R}_+, (1+x)\mathrm{d}x) \times \mathbb{R}_+$ *and assuming hypotheses* (H1)–(H3)*, Lifshitz–Slyozov system* (11) *has a unique solution on the interval* $[0, T]$ *in the sense of Def.* 2.3.

Note that the mild solution given by Theorem 2.3 is also a weak solution in the sense of Definition 2.2, see Calvo et al. (2021), and under hypotheses (H1)–(H3) both definitions coincide.

3 A new convergence result from Becker–Döring to Lifshitz–Slyozov equations

In this part of our work we introduce a different way to see the convergence from the Becker–Döring equations to the Lifshitz–Slyozov equations. Using tail distributions

allows to reduce the non linearity of our system by pulling the speed of advection outside of the space derivative. Tail distributions were also found to be useful to obtain a quasi comparison principle in Cañizo et al. (Aug. 2019) and to obtain refined uniqueness properties in Laurençot (2001); Calvo et al. (2021). The main idea is to use results on the tail of the distributions to show convergence. Finally, we note that our result uses the fact that a solution to system (11) exists while the previous result also shows existence of solution of (11), by showing a convergence to a measure valued function which turns out to be a solution of (11).

Let $(f^\varepsilon, L^\varepsilon)$ be the solution of the Becker–Döring ODE system (14) and Eq. (19), and let (f, L) the mild solution of Lifshitz–Slyozov equations (11). We recall the tail distribution definition,

$$F(t,x) = \int_x^\infty f(t,y)\mathrm{d}y, \qquad F^\varepsilon(t,x) = \int_x^\infty f^\varepsilon(t,y)\mathrm{d}y, \tag{21}$$

and introduce their difference

$$E(t,x) = F^\varepsilon(t,x) - F(t,x). \tag{22}$$

We introduce the following additional hypotheses to use in our main theorem:

$$\sup_{x\in\mathbb{R}_+} |a''(x)| < +\infty \text{ and } \sup_{x\in\mathbb{R}_+} |b''(x)| < +\infty, \tag{H5}$$

$$\sum_{i\geq 0} |c_{i+1}^{\varepsilon,0} - c_i^{\varepsilon,0}| < +\infty, \text{ uniformly in } \varepsilon, \tag{H6}$$

$$\varepsilon \sum_{i\geq 0} i\,|c_{i+1}^{\varepsilon,0} - c_i^{\varepsilon,0}| < +\infty, \text{ uniformly in } \varepsilon. \tag{H7}$$

$$\text{There exists some constant } \bar{L} > 0 \text{ independent of } \varepsilon, \text{ such that } \inf_{\varepsilon>0} L^{\varepsilon,0} \geq \bar{L}. \tag{H8}$$

$$\text{There exists some constant } K > 0 \text{ independent of } \varepsilon, \text{ such that } \sup_{\varepsilon>0} c_0^{\varepsilon,0} < K. \tag{H9}$$

We now state our main theorem.

Theorem 3.1 *Let $T > 0$ and denote $E(t,x) = F^\varepsilon(t,x) - F(t,x)$, see Eq. (22). Suppose that there exists some constant $C_{\text{init}} > 0$ such that for all $\varepsilon > 0$, $\int_{\mathbb{R}_+} |E(0,x)|\mathrm{d}x \leq \varepsilon C_{\text{init}}$. Also assume that hypotheses (H1)–(H9) hold true. Then there exists some constants $C(T) > 0$ (independent of ε) and ε^* (independent of T) and such that for all $0 < \varepsilon \leq \varepsilon^*$ and for all $t \in (0,T]$:*

$$|L^\varepsilon(t) - L(t)| + \int_{\mathbb{R}_+} |E(t,x)|\mathrm{d}x \leq \varepsilon C(T).$$

The proof proceeds as follows. Taking inspiration from Laurençot (2001); Calvo et al. (2021), we first note that owing to the total population number conservation, the lipid terms can be controlled by the tail, $|L^\varepsilon(t) - L(t)| \leq \int_{\mathbb{R}_+} |E(t,x)|\mathrm{d}x$. The control on the tail relies on a Grönwall's lemma argument. For that purpose, we derive the equation followed by $F^\varepsilon(t,x)$ (Lemma 3.5). We point out that the case $x < \varepsilon/2$ has to be treated separately due to remaining boundary terms. This allows us to give a first estimate on the integral $\int_{\mathbb{R}_+} |E(t,x)|\mathrm{d}x$. We then make use of the mild solution formulation to derive the partial differential equation followed by F and in turn the one followed by E (Lemma 3.6). The proof follows by bounding the terms in the estimate on $\int_{\mathbb{R}_+} |E(t,x)|\mathrm{d}x$, and in particular we show that $F^\varepsilon(t,x)$ satisfies the same equation as F up to an order ε (Lemma 3.7). To this end, the key argument relies on refined estimates of the difference between the first order derivative of $F^\varepsilon(t,x)$ and its discrete analog. This estimate needs uniform control on the solutions c_i^ε of the Becker–Döring system and their increments $c_{i+1}^\varepsilon - c_i^\varepsilon$ (Sect. 3.1, Lemmas 3.1 to 3.4), which is new, up to our knowledge.

Hypotheses (H1)–(H4) are classical in the study of our model. However, other assumptions are less common but arise naturally from the result. Contrary to the classical convergence result, we work with mild solutions of the Lifshitz–Slyozov system. Hence, we need proper bounds on second order terms. We shall see in Sect. 4 that those terms lead us to the second order Lifshitz–Syozov model. Nonetheless, those terms involve second order derivatives of both a and b which leads us to hypothesis (H5). Hypotheses (H6) and (H7) simply tell us that the initial condition for the Becker–Döring system must have finite zeroth order moment and first moment increments independently of ε. Lemma 3.4 shows that this property propagates in time. Additional assumptions have to be made to obtain our main theorem. The assumption (H8) on the initial condition $L^{\varepsilon,0}$ is necessary since it leads to strict positivity of L^ε in finite time, uniformly in ε. The assumption (H9) on the initial condition $c_0^{\varepsilon,0}$ is technical and ensures that the proper boundary condition (11c) is satisfied for all times. Finally the assumption on $\displaystyle\int_{\mathbb{R}_+} |E(0,x)|\mathrm{d}x$ is made to conclude after using Grönwall's lemma at the very end of the proof. This assumption relates both initial conditions $(c_i^{\varepsilon,0})_{i\geq 0}$ and f^0. A fair choice for the initial condition $(c_i^{\varepsilon,0})_{i\geq 0}$ is $c_i^{\varepsilon,0} = f^0(i\varepsilon)$ for all $i \geq 0$. Then the assumption is verified as long as $(f^0)' \in L^1(\mathbb{R}_+, x\mathrm{d}x)$.

In all this section, we assume that hypotheses (H1)–(H9) hold true.

3.1 Preliminary results on Becker–Döring system

We start with a lemma that allows to control the lipid term away from 0, in the lines of previous results from Calvo et al. (2021).

Lemma 3.1 *A solution $(L^\varepsilon, c^\varepsilon)$ of (14) with $\lambda > 0$ independent of ε verifies that there exists $C > 0$ independent of ε, such that for all $t > 0$,*

$$\inf_{\varepsilon>0} L^\varepsilon(t) \geq \bar{L}\exp(-Ct), \tag{23}$$

where $\bar{L}$ is defined at (H8).

Proof For all $t > 0$, we have, using the three first equations of system (14):

$$\frac{\mathrm{d}L^\varepsilon(t)}{\mathrm{d}t} = -\varepsilon \sum_{i\geq 0} J_i^\varepsilon(c^\varepsilon(t), L^\varepsilon(t)) = -\varepsilon \sum_{i\geq 0} \left(a_i^\varepsilon \frac{L^\varepsilon(t)}{L^\varepsilon(t)+\kappa} c_i^\varepsilon(t) - b_{i+1}^\varepsilon c_{i+1}\varepsilon(t) \right)$$
$$\geq -\frac{L^\varepsilon(t)}{L^\varepsilon(t)+\kappa} \varepsilon \sum_{i\geq 0} a_i^\varepsilon c_i^\varepsilon(t),$$

and thus, because $\sup_{x\in\mathbb{R}_+} |a(x)| = C_a$, and $\frac{L^\varepsilon}{L^\varepsilon+\kappa} \leq \frac{1}{\kappa} L^\varepsilon$:

$$\frac{\mathrm{d}L^\varepsilon(t)}{\mathrm{d}t} \geq -\frac{C_a}{\kappa} L^\varepsilon \int_{-\varepsilon/2}^{+\infty} f^\varepsilon(t,x)\mathrm{d}x$$

and by conservation of the moment (15), $\int_{-\varepsilon/2}^{+\infty} f^\varepsilon(t,x)\mathrm{d}x = \varepsilon \sum_{i\geq 0} c_i^\varepsilon(t) = m$,

$$\frac{\mathrm{d}L^\varepsilon(t)}{\mathrm{d}t} \geq -\frac{C_a m}{\kappa} L^\varepsilon.$$

We conclude by Grönwall's lemma and using Hypothesis (H8). □

We next state a lemma adapted from Deschamps et al. (2017) that allows to obtain pointwise estimates of the density f^ε near the boundary, through the uniform propagation of exponential moments. For $x \in \mathbb{R}_+$ and $t > 0$, let

$$H^\varepsilon(t,x) = \sum_{i\geq 0} c_i^\varepsilon(t) \mathrm{e}^{-ix}.$$

Lemma 3.2 *Let $x \in \mathbb{R}_+^*$. Then there exist some constants $\varepsilon^* > 0$ and $\tilde{K} > 0$ independent of ε^*, such that for all $0 < \varepsilon < \varepsilon^*$:*

$$H^\varepsilon(t,x) \leq H^\varepsilon(0,x) + \tilde{K} \text{ for all } t > 0,$$

and in particular:

$$\text{for all } i \geq 0, \quad \sup_{0<\varepsilon<\varepsilon^*} \sup_{t\in[0,T]} c_i^\varepsilon(t) \leq \bar{c}_i < +\infty. \tag{24}$$

Proof Using Lemma 3.1, and the assumption (H8) on $L^\varepsilon(0)$, we have that $\inf_{\varepsilon>0} \inf_{t\in(0,T]} L^\varepsilon(t) \geq \bar{L}\exp(-CT)$. Thus we can find a constant $c > 0$ such that:

$$\inf_{\varepsilon>0} \inf_{t\in(0,T]} \frac{L^\varepsilon(t)}{L^\varepsilon(t)+\kappa} \geq c.$$

Now we choose $\delta > 0$ such that $c > 2\delta$. Using Taylor's expansion, we have $a(i\varepsilon) = a(0) + i\varepsilon a'(0) + \mathcal{O}((i\varepsilon)^2)$. Then with hypotheses (H2b) and (H3) and for ε small enough, we find that $a(i\varepsilon) \geq \frac{3}{4}(a(0) - i\varepsilon K_a) > 0$. Therefore we have that for ε small enough:

$$\forall i \leq \frac{1}{\sqrt{\varepsilon}},\ a(i\varepsilon) \geq \frac{a(0)}{2}. \tag{25}$$

In turn, by hypotheses (H2a), (H2b) and (H4), we have that for ε small enough and for all $i \leq \frac{1}{\sqrt{\varepsilon}}$:

$$\frac{b_i^\varepsilon}{a_i^\varepsilon} = \frac{b(i\varepsilon)}{a(i\varepsilon)} \leq 2C_b \frac{\sqrt{\varepsilon}}{a(0)} \xrightarrow[\varepsilon\to 0]{} 0.$$

Let $x \in \mathbb{R}_+^*$. Hence, one can find $\varepsilon^* > 0$ such that:

$$\sup_{\varepsilon<\varepsilon^*} \sup_{i\leq\frac{1}{\sqrt{\varepsilon}}} \left|\frac{b_i^\varepsilon}{a_i^\varepsilon}\right| \leq \delta\, \mathrm{e}^{-x}.$$

This gives us that for ε^* small enough, $\varepsilon < \varepsilon^*$ and $i \leq \frac{1}{\sqrt{\varepsilon}}$:

$$\frac{L^\varepsilon(t)}{L^\varepsilon(t)+\kappa} - \frac{b_i^\varepsilon}{a_i^\varepsilon}\mathrm{e}^x \geq 2\delta - \delta = \delta. \tag{26}$$

Now we proceed with the bound on H^ε using Eqs. (14) and (12):

$$\begin{aligned}\varepsilon\partial_t H^\varepsilon(t,x) &= (\mathrm{e}^{-x}-1)\sum_{i\geq 0} J_i^\varepsilon(c)\,\mathrm{e}^{-ix} \\ &= (\mathrm{e}^{-x}-1)\left[\frac{L^\varepsilon(t)}{L^\varepsilon(t)+\kappa}a_0^\varepsilon c_0^\varepsilon(t) + \sum_{i\geq 1} a_i^\varepsilon\left(\frac{L^\varepsilon(t)}{L^\varepsilon(t)+\kappa} - \frac{b_i^\varepsilon}{a_i^\varepsilon}\mathrm{e}^x\right)c_i^\varepsilon(t)\,\mathrm{e}^{-ix}\right].\end{aligned}$$

Now we split the sum on the right depending on $\frac{1}{\sqrt{\varepsilon}}$ with ε small enough as before. Note that since $x > 0$, we have that $(\mathrm{e}^{-x}-1) < 0$. The first sum is treated using (26) and the bound (25):

$$\varepsilon\partial_t H^\varepsilon(t,x) \leq (\mathrm{e}^{-x}-1)\left[2\delta a_0^\varepsilon c_0^\varepsilon(t) + \frac{a(0)}{2}\delta\sum_{i=1}^{\lfloor\frac{1}{\sqrt{\varepsilon}}\rfloor} c_i^\varepsilon(t)\,\mathrm{e}^{-ix} - \mathrm{e}^x \sum_{i\geq\lfloor\frac{1}{\sqrt{\varepsilon}}\rfloor+1} b_i^\varepsilon c_i^\varepsilon(t)\,\mathrm{e}^{-ix}\right].$$

The term in c_0^ε and the first sum are combined and using our choice of δ, it yields:

$$2\delta a_0^\varepsilon c_0^\varepsilon(t) + \frac{a(0)}{2}\delta \sum_{i=1}^{\lfloor \frac{1}{\sqrt{\varepsilon}} \rfloor} c_i^\varepsilon(t)\,\mathrm{e}^{-ix} \geq \frac{a(0)}{2}\delta \left(H^\varepsilon(t,x) - \sum_{i \geq \lfloor \frac{1}{\sqrt{\varepsilon}} \rfloor + 1} c_i^\varepsilon(t)\,\mathrm{e}^{-ix} \right).$$

Hence:

$$\begin{aligned} &\varepsilon \partial_t H^\varepsilon(t,x) \\ &\leq (1-\mathrm{e}^{-x}) \left[\frac{a(0)}{2}\delta \left(-H^\varepsilon(t,x) + \sum_{i \geq \lfloor \frac{1}{\sqrt{\varepsilon}} \rfloor + 1} c_i^\varepsilon(t)\,\mathrm{e}^{-ix} \right) + \mathrm{e}^{x} \sum_{i \geq \lfloor \frac{1}{\sqrt{\varepsilon}} \rfloor + 1} b_i^\varepsilon c_i^\varepsilon(t)\,\mathrm{e}^{-ix} \right]. \end{aligned}$$

Observe that for ε small enough depending on x, for all $i \geq \lfloor \frac{1}{\sqrt{\varepsilon}} \rfloor$, we have:

$$(\delta \frac{a(0)}{2} + \mathrm{e}^{x}\, b_i^\varepsilon)\,\mathrm{e}^{-ix} \leq K(C_a + C_b)(1 + i\varepsilon)\,\mathrm{e}^{-ix} \leq K\varepsilon,$$

which leads to:

$$\varepsilon \partial_t H^\varepsilon(t,x) \leq \frac{a(0)}{2}\delta(\mathrm{e}^{-x} - 1) H^\varepsilon(t,x) + (1-\mathrm{e}^{-x}) K m.$$

We conclude by using Grönwall's lemma and $\tilde{K} = \frac{2Km}{\delta a(0)}$ and (24) follows immediately. □

A direct consequence of Lemma 3.2 is the following refined estimate on c_0^ε which shows that at the limit $\varepsilon \to 0$, the density f^ε vanishes at the boundary, in agreement with the limiting boundary condition (11c):

Lemma 3.3 *There exist constants $C_1, C_2 > 0$ independent of ε such that for ε small enough and for all $t \in (0, T]$:*

$$c_0^\varepsilon(t) \leq \mathrm{e}^{-\frac{C_1}{\varepsilon} t}\, c_0^{\varepsilon,0} + \varepsilon C_2. \tag{27}$$

Proof As in the proof of Lemma 3.2, there exists ε small enough such that:

$$\frac{\mathrm{d}c_0^\varepsilon(t)}{\mathrm{d}t} = \frac{1}{\varepsilon}(b_1^\varepsilon c_1^\varepsilon(t) - a_0^\varepsilon \frac{L^\varepsilon(t)}{L^\varepsilon(t) + \kappa} c_0^\varepsilon(t)) \leq C_b \bar{c_1} - \frac{a(0)}{\varepsilon}\delta c_0^\varepsilon(t),$$

thanks to hypothesis (H'1). Now applying Grönwall's lemma, we obtain:

$$c_0^\varepsilon(t) \leq \mathrm{e}^{-\frac{a(0)\delta t}{\varepsilon}}\, c_0^\varepsilon(0) + C_b \bar{c_1} \frac{\varepsilon}{\delta a(0)} (1 - \mathrm{e}^{-\frac{a(0)}{\varepsilon}\delta t}),$$

which gives the desired result. □

We end this section by a last lemma that will be useful to control the first spatial derivative of F^ε.

Lemma 3.4 *For all $T > 0$, there exist constants C_3 and C_4 independent of ε such that for ε small enough,*

$$\sup_{t\le T}\sum_{i\ge 0}|c_{i+1}^\varepsilon - c_i^\varepsilon|(t) < C_3, \tag{28}$$

$$\sup_{t\le T}\varepsilon\sum_{i\ge 0} i|c_{i+1}^\varepsilon - c_i^\varepsilon|(t) < C_4. \tag{29}$$

Proof Let $u_i = c_{i+1}^\varepsilon - c_i^\varepsilon$ and let's estimate its time derivative. Then, for all $i \ge 1$, we have from Eqs. (14) and (12):

$$\begin{aligned}
\frac{\mathrm{d}u_i}{\mathrm{d}t} =& \frac{L^\varepsilon(t)}{L^\varepsilon(t)+\kappa}\left(\frac{a_{i-1}^\varepsilon}{\varepsilon}u_{i-1} - \frac{a_{i-1}^\varepsilon - a_i^\varepsilon}{\varepsilon}c_i^\varepsilon - \frac{a_i^\varepsilon}{\varepsilon}u_i - \frac{a_{i+1}^\varepsilon - a_i^\varepsilon}{\varepsilon}c_{i+1}^\varepsilon\right)\\
&- \left(\frac{b_i^\varepsilon}{\varepsilon}u_i - \frac{b_{i+1}^\varepsilon + b_i^\varepsilon}{\varepsilon}c_{i+1}^\varepsilon - \frac{b_{i+1}^\varepsilon}{\varepsilon}u_{i+1} + \frac{b_{i+1}^\varepsilon - b_{i+2}^\varepsilon}{\varepsilon}c_{i+2}^\varepsilon\right)\\
=& \frac{J_{i-1}^\varepsilon(u,L^\varepsilon) - J_i^\varepsilon(u,L^\varepsilon)}{\varepsilon}\\
&+ \frac{L^\varepsilon(t)}{L^\varepsilon(t)+\kappa}\left(\frac{a_{i-1}^\varepsilon - a_i^\varepsilon}{\varepsilon}u_i - \left(\frac{a_{i-1}^\varepsilon - a_i^\varepsilon}{\varepsilon} + \frac{a_{i+1}^\varepsilon - a_i^\varepsilon}{\varepsilon}\right)c_{i+1}^\varepsilon\right)\\
&+ \frac{b_{i+1}^\varepsilon - b_i^\varepsilon}{\varepsilon}u_{i+1} + \left(\frac{b_{i+1}^\varepsilon - b_i^\varepsilon}{\varepsilon} + \frac{b_{i+1}^\varepsilon - b_{i+2}^\varepsilon}{\varepsilon}\right)c_{i+2}^\varepsilon.
\end{aligned}$$

We multiply the previous expression for $i \ge 1$ by $\mathrm{sign}(u_i)$ on both sides, which gives:

$$\begin{aligned}
\frac{\mathrm{d}|u_i|}{\mathrm{d}t} \le& \frac{J_{i-1}^\varepsilon(|u|,L^\varepsilon) - J_i^\varepsilon(|u|,L^\varepsilon)}{\varepsilon} + \frac{|a_{i-1}^\varepsilon - a_i^\varepsilon|}{\varepsilon}|u_i| + \frac{|a_{i-1}^\varepsilon - 2a_i^\varepsilon + a_{i+1}^\varepsilon|}{\varepsilon}c_{i+1}^\varepsilon\\
&+ \frac{|b_{i+1}^\varepsilon - b_i^\varepsilon|}{\varepsilon}|u_{i+1}| + \frac{|b_{i+2}^\varepsilon - 2b_{i+1}^\varepsilon + b_i^\varepsilon|}{\varepsilon}c_{i+2}^\varepsilon.
\end{aligned}$$

Hence, thanks to hypotheses (H3) and (H5) and Lemma 3.2, there exists ε small enough such that for $i \ge 1$:

$$\begin{aligned}
\frac{\mathrm{d}|u_i|}{\mathrm{d}t} \le& \frac{J_{i-1}^\varepsilon(|u|,L^\varepsilon) - J_i^\varepsilon(|u|,L^\varepsilon)}{\varepsilon} + \|a'\|_\infty|u_i| + \varepsilon\|a''\|_\infty c_{i+1}^\varepsilon\\
&+\|b'\|_\infty|u_{i+1}| + \varepsilon\|b''\|_\infty c_{i+2}^\varepsilon.
\end{aligned} \tag{30}$$

Now, for $i = 0$, we obtain:

$$\begin{aligned}
\frac{\mathrm{d}u_0}{\mathrm{d}t} =& -\frac{1}{\varepsilon}J_0^\varepsilon(u,L^\varepsilon) - \frac{a_1^\varepsilon - a_0^\varepsilon}{\varepsilon}\frac{L^\varepsilon(t)}{L^\varepsilon(t)+\kappa}c_1^\varepsilon + \frac{a_0^\varepsilon}{\varepsilon}\frac{L^\varepsilon(t)}{L^\varepsilon(t)+\kappa}c_0^\varepsilon\\
&+ \frac{b_2^\varepsilon - b_1^\varepsilon}{\varepsilon}c_2^\varepsilon - \frac{b_1^\varepsilon}{\varepsilon}c_1^\varepsilon.
\end{aligned}$$

Since $b_0^\varepsilon = b(0) = 0$, we can treat the remaining terms in b as before by adding and removing the right terms for free. The terms with c_1^ε are bounded using Lemma 3.2 and the one with c_0^ε using Lemma 3.3. Hence, there exists ε small enough such that:

$$\frac{\mathrm{d}|u_0|}{\mathrm{d}t} \leq -\frac{1}{\varepsilon} J_0^\varepsilon(|u|, L^\varepsilon) + \|a'\|_\infty \bar{c_1} + \frac{a(0)}{\varepsilon} \mathrm{e}^{-\frac{C_1}{\varepsilon}t} c_0^{\varepsilon,0} + a(0)C_2 + \|b'\|_\infty |u_1| + \varepsilon \|b''\|_\infty c_2^\varepsilon.$$

We sum the previous estimates for all $i \geq 0$ and we get:

$$\begin{aligned}\frac{\mathrm{d}}{\mathrm{d}t} \sum_{i\geq 0} |u_i| &\leq (\|a'\|_\infty + \|b'\|_\infty) \sum_{i\geq 0} |u_i| \\ &+ (\|a''\|_\infty + \|b''\|_\infty)\varepsilon \sum_{i\geq 0} c_i^\varepsilon + \|a'\|_\infty \bar{c_1} + \frac{a(0)}{\varepsilon} \mathrm{e}^{-\frac{C_1}{\varepsilon}t} c_0^{\varepsilon,0} + a(0)C_2.\end{aligned}$$

We integrate the previous inequality over $[0, t]$, for $0 < t < T$:

$$\begin{aligned}\sum_{i\geq 0} |u_i|(t) \leq \sum_{i\geq 0} |u_i|(0) &+ (\|a'\|_\infty + \|b'\|_\infty) \int_0^t \sum_{i\geq 0} |u_i|(s)\mathrm{d}s \\ &+ (\|a''\|_\infty + \|b''\|_\infty) mT + \frac{a(0)}{C_1} c_0^{\varepsilon,0} + (a(0)C_2 + \|a'\|_\infty \bar{c_1})T.\end{aligned}$$

And finally Grönwall's lemma yields:

$$\sum_{i\geq 0} |u_i|(t) \leq C_u(T)$$

with

$$\begin{aligned}C_u(T) = &\left(\sum_{i\geq 0} |u_i|(0) + (\|a''\|_\infty + \|b''\|_\infty) mT + \frac{a(0)}{C_1} c_0^{\varepsilon,0} + (a(0)C_2 + \|a'\|_\infty \bar{c_1})T \right) \\ &\times \exp((\|a'\|_\infty + \|b'\|_\infty)T),\end{aligned}$$

which gives Eq. (28).

Using the definition (14c) of λ, estimate (30) and hypothesis (H'1), we obtain the following inequalities:

$$\begin{aligned}\varepsilon \frac{\mathrm{d}}{\mathrm{d}t} \sum_{i\geq 1} i|u_i| &\leq \varepsilon \sum_{i\geq 1} i \frac{J_{i-1}^\varepsilon(|u|) - J_i^\varepsilon(|u|)}{\varepsilon} + \varepsilon(\|a'\|_\infty + \|b'\|_\infty) \sum_{i\geq 1} i|u_i| \\ &\quad + (\|a''\|_\infty + \|b''\|_\infty)\varepsilon^2 \sum_{i\geq 0} i c_i^\varepsilon \\ &\leq \sum_{i\geq 0} J_i^\varepsilon(|u|) + (\|a'\|_\infty + \|b'\|_\infty)\varepsilon \sum_{i\geq 1} i|u_i| + (\|a''\|_\infty + \|b''\|_\infty)\lambda \\ &\leq C_a \sum_{i\geq 0} |u_i| + (\|a'\|_\infty + \|b'\|_\infty)\varepsilon \sum_{i\geq 1} i|u_i| + (\|a''\|_\infty + \|b''\|_\infty)\lambda.\end{aligned}$$

Integrating over $[0, t]$ and using the previous bound on $\sum_{i\geq 0}|u_i|$, we conclude using Grönwall's lemma:

$$\varepsilon\sum_{i\geq 1} i|u_i|(t) \leq \left(\varepsilon\sum_{i\geq 1} i|u_i|(0) + C_a C_u(T)T + (\|a''\|_\infty + \|b''\|_\infty)\lambda T\right) \exp((\|a'\|_\infty + \|b'\|_\infty)T),$$

which yields Eq. (29). □

3.2 Proof of theorem 3.1

In this section, we make use of the lemmas from the previous section. As such, from then on, ε is taken small enough to apply those lemmas. We first derive the equation satisfied by the tail distribution F^ε defined at Eq. (21). Recall that operator Δ_ε is defined at Eq. (20).

Lemma 3.5 *For all $x \geq \frac{\varepsilon}{2}$ and $t \geq 0$:*

$$\partial_t F^\varepsilon(t,x) = \frac{1}{\varepsilon}\int_{x-\varepsilon}^{x}(a^\varepsilon(y)\frac{L^\varepsilon(t)}{L^\varepsilon(t)+\kappa} - a(x)\frac{L(t)}{L(t)+\kappa})f^\varepsilon(t,y)\mathrm{d}y - a(x)\frac{L(t)}{L(t)+\kappa}\Delta_{-\varepsilon}F^\varepsilon(t,x) - \frac{1}{\varepsilon}\int_{x}^{x+\varepsilon}(b^\varepsilon(y)-b(x))f^\varepsilon(t,y)\mathrm{d}y + b(x)\Delta_\varepsilon F^\varepsilon(t,x) \quad (31)$$

and for all $x < \frac{\varepsilon}{2}$ and $t \geq 0$:

$$\partial_t F^\varepsilon(t,x) = \frac{1}{\varepsilon}\int_{-\frac{\varepsilon}{2}}^{x} a^\varepsilon(y)\frac{L^\varepsilon(t)}{L^\varepsilon(t)+\kappa}f^\varepsilon(t,y)\mathrm{d}y - \frac{1}{\varepsilon}\int_{\frac{\varepsilon}{2}}^{x+\varepsilon} b^\varepsilon(y)f^\varepsilon(t,y)\mathrm{d}y. \quad (32)$$

Remark The function f^ε is defined on $[-\frac{\varepsilon}{2}, +\infty[$ whereas f is defined on $\mathbb{R}_+$. However we will only concern ourselves with $x \in \mathbb{R}_+$ in the following subsections. Hence we will treat the case $x < \varepsilon/2$ independently to accommodate for boundary terms that might be left off from f^ε. We also point out that:

$$\int_0^{+\infty} f^\varepsilon(t,x)\mathrm{d}x = m - \frac{\varepsilon}{2}c_0^\varepsilon(t) \quad (33)$$

Owing to Lemma 3.2, the right hand side is bounded and tends to m as $\varepsilon \to 0$.And for the first order we have an exact computation:

$$L^\varepsilon(t) + \int_0^{+\infty} x f^\varepsilon(t,x)\mathrm{d}x = \lambda \quad (34)$$

Proof For all $x \in \mathbb{R}_+$ and $t \in [0, T]$, it comes directly from the definitions (20) and (21) that the following equations hold true:

for all $x \geq 0$ and $t \geq 0$,

$$\Delta_\varepsilon F^\varepsilon(t,x) = -\frac{1}{\varepsilon}\int_x^{x+\varepsilon} f^\varepsilon(t,y)\mathrm{d}y, \tag{35}$$

and for all $x \geq \frac{\varepsilon}{2}$ and $t \geq 0$,

$$\Delta_{-\varepsilon} F^\varepsilon(t,x) = -\frac{1}{\varepsilon}\int_{x-\varepsilon}^{x} f^\varepsilon(t,y)\mathrm{d}y. \tag{36}$$

Denote $H_x = \mathbb{1}_{[x,+\infty)}$. First observe that:

$$\Delta_\varepsilon H_x(y) = \frac{1}{\varepsilon}\left(\mathbb{1}_{[x,+\infty)}(y+\varepsilon) - \mathbb{1}_{[x,+\infty)}(y)\right) = \frac{1}{\varepsilon}\mathbb{1}_{[x-\varepsilon,x)}(y),$$
$$\Delta_{-\varepsilon} H_x(y) = \frac{1}{\varepsilon}\mathbb{1}_{[x,x+\varepsilon)}(y).$$

Then we use Proposition 2.2 for the Heaviside function. It yields that for all $x \geq \frac{\varepsilon}{2}$:

$$\begin{aligned}
\partial_t F^\varepsilon(t,x) &= \int_{\mathbb{R}_+} H_x(y)\partial_t f^\varepsilon(t,y)\mathrm{d}y \\
&= \int_{\mathbb{R}_+}\left(\Delta_\varepsilon H_x(y)a^\varepsilon(y)\frac{L^\varepsilon(t)}{L^\varepsilon(t)+\kappa} - \Delta_{-\varepsilon}H_x(y)b^\varepsilon(y)\right) f^\varepsilon(t,y)\mathrm{d}y \\
&= \int_{x-\varepsilon}^{x}\frac{1}{\varepsilon}a^\varepsilon(y)\frac{L^\varepsilon(t)}{L^\varepsilon(t)+\kappa}f^\varepsilon(t,y)\mathrm{d}y - \int_x^{x+\varepsilon}\frac{1}{\varepsilon}b^\varepsilon(y)f^\varepsilon(t,y)\mathrm{d}y \\
&= \frac{1}{\varepsilon}\int_{x-\varepsilon}^{x}\Big(a^\varepsilon(y)\frac{L^\varepsilon(t)}{L^\varepsilon(t)+\kappa} \\
&\quad - a(x)\frac{L(t)}{L(t)+\kappa}\Big)f^\varepsilon(t,y)\mathrm{d}y - a(x)\frac{L(t)}{L(t)+\kappa}\Delta_{-\varepsilon}F^\varepsilon(t,x) \\
&\quad - \frac{1}{\varepsilon}\int_x^{x+\varepsilon}(b^\varepsilon(y)-b(x))f^\varepsilon(t,y)\mathrm{d}y + b(x)\Delta_\varepsilon F^\varepsilon(t,x)
\end{aligned}$$

The case for $x < \frac{\varepsilon}{2}$ follows from simple computation, using that $\int_{-\varepsilon/2}^{+\infty} f^\varepsilon(t,x)\mathrm{d}x = m$ by conservation of the moment (15):

$$\begin{aligned}
\partial_t F^\varepsilon(t,x) &= \frac{\mathrm{d}}{\mathrm{d}t}\int_{\frac{-\varepsilon}{2}}^{+\infty} f^\varepsilon(t,y)\mathrm{d}y - \frac{\mathrm{d}}{\mathrm{d}t}\int_{\frac{-\varepsilon}{2}}^{x} f^\varepsilon(t,y)\mathrm{d}y = -(x+\frac{\varepsilon}{2})\frac{\mathrm{d}}{\mathrm{d}t}c_0^\varepsilon(t) \\
&= \frac{1}{\varepsilon}\int_{\frac{-\varepsilon}{2}}^{x} a^\varepsilon(y)\frac{L^\varepsilon(t)}{L^\varepsilon(t)+\kappa}f^\varepsilon(t,y)\mathrm{d}y - \frac{1}{\varepsilon}\int_{\frac{\varepsilon}{2}}^{x+\varepsilon} b^\varepsilon(y)f^\varepsilon(t,y)\mathrm{d}y.
\end{aligned}$$

□

We then derive an upper bound for the time derivative of $\int_{\mathbb{R}_+} |E(t,x)|\mathrm{d}x$, where E is defined at Eq. (22).

Lemma 3.6 *For all $t \geq 0$, we have:*

$$\begin{aligned}\frac{d}{\mathrm{d}t}\int_{\mathbb{R}_+}|E(t,x)|\mathrm{d}x &\leq (\|a'\|_\infty + \|b'\|_\infty)\int_{\mathbb{R}_+}|E(t,x)|\mathrm{d}x\\ &+\int_{\mathbb{R}_+}|\partial_t F^\varepsilon(t,x) + v(x,L(t))\partial_x F^\varepsilon(t,x)|\mathrm{d}x\\ &+\frac{\varepsilon}{2}a(0)\frac{L(t)}{L(t)+\kappa}c_0^\varepsilon(t).\end{aligned} \tag{37}$$

Proof From the definitions of the tail distributions in Eq. (21), the following equations hold true:

$$\begin{aligned}&\partial_x F(t,x) = -f(t,x),\\ &\partial_x F^\varepsilon(t,x) = -f^\varepsilon(t,x), \text{ a.e. in } \mathbb{R}_+.\end{aligned}$$

By Def.2.3, we have:

$$\begin{aligned}F(t,x) &= \int_{\max(x,X_c(t))}^{+\infty} f^0(X(0;t,y))\partial_y X(0;t,y)\mathrm{d}y\\ &= \begin{cases}\int_0^{+\infty} f^0(y)\mathrm{d}y & \text{if } x \leq X_c(t),\\ \int_{X(0;t,x)}^{+\infty} f^0(y)\mathrm{d}y & \text{if } x \geq X_c(t).\end{cases}\end{aligned}$$

Therefore if $x \leq X_c(t)$, then $\partial_t F(t,x) = 0 = \partial_x F(t,x)$. And if $x \geq X_c(t)$, the following expressions hold:

$$\begin{aligned}\partial_t F(t,x) &= -f^0(X(0;t,x))\partial_t X(0;t,x),\\ \partial_x F(t,x) &= -f^0(X(0;t,x))\partial_x X(0;t,x) = -f(t,x).\end{aligned}$$

By properties of characteristics we have: $\partial_t X(0;t,x) + v(x,L)\partial_x X(0;t,x) = 0$ and thus:

$$\begin{aligned}&\partial_t F(t,x) + v(x,L(t))\partial_x F(t,x)\\ &\quad = -f^0(X(0;t,x))(\partial_t X(0;t,x) + v(x,L)\partial_x X(0;t,x)) = 0.\end{aligned}$$

We then compute:

$$\begin{aligned}\partial_t E(t,x) &= \partial_t F^\varepsilon(t,x) - \partial_t F(t,x)\\ &= -v(x,L(t))\partial_x(F^\varepsilon - F)(t,x) + \partial_t F^\varepsilon(t,x) + v(x,L(t))\partial_x F^\varepsilon(t,x).\end{aligned}$$

We integrate the previous equality, we use the definition (46) of v with hypothesis (H3) and we find:

$$\begin{aligned}\frac{\mathrm{d}}{\mathrm{d}t}\int_{\mathbb{R}_+}|E|\mathrm{d}x &= -\int_{\mathbb{R}_+} v\partial_x|E|\mathrm{d}x + \int_{\mathbb{R}_+}\mathrm{sign}(E)(\partial_t F^\varepsilon + v(x,L(t))\partial_x F^\varepsilon)\mathrm{d}x\\ &= -[v(x,L(t))|E(t,x)|]_0^{+\infty} + \int_{\mathbb{R}_+}\partial_x v|E|\mathrm{d}x + \int_{\mathbb{R}_+}\mathrm{sign}(E)(\partial_t F^\varepsilon + v\partial_x F^\varepsilon)\mathrm{d}x\\ &\le v(0,L(t))|E(t,0)| + (\|a'\|_\infty + \|b'\|_\infty)\int_{\mathbb{R}_+}|E|\mathrm{d}x + \int_{\mathbb{R}_+}|\partial_t F^\varepsilon + v\partial_x F^\varepsilon|\mathrm{d}x\\ &= (\|a'\|_\infty + \|b'\|_\infty)\int_{\mathbb{R}_+}|E|\mathrm{d}x + \int_{\mathbb{R}_+}|\partial_t F^\varepsilon + v\partial_x F^\varepsilon|\mathrm{d}x + \frac{\varepsilon}{2}a(0)\frac{L(t)}{L(t)+\kappa}c_0^\varepsilon(t).\end{aligned}$$

The last equality is obtained since $b(0) = 0$ and $|E(t,0)| = |\int_{\mathbb{R}_+}(f^\varepsilon - f)(t,x)\mathrm{d}x| = \frac{\varepsilon}{2}c_0^\varepsilon(t)$, see Eq. (33). □

Thanks to the equation on F^ε given by Lemma 3.5, we control the second term in Eq. (37) in the next lemma.

Lemma 3.7 *There exist some constants $C_1, C_2 > 0$ independent of ε such that for all $t \in (0,T]$:*

$$\int_{\mathbb{R}_+}|(\partial_t F^\varepsilon + v\partial_x F^\varepsilon)(t,x)|\mathrm{d}x \le \varepsilon C_1 + C_2|L^\varepsilon(t) - L(t)|. \tag{38}$$

Proof First by construction of both a^ε and b^ε, and the fact that a and b are lipshitz continuous, one has for all $x, y \in \mathbb{R}_+$ such that $|y - x| \le \varepsilon$:

$$\left|\frac{a^\varepsilon(y) - a(x)}{\varepsilon}\right| \le 2\|a'\|_\infty$$

and similarly for b^ε. Also observe that the derivative of $x \to \frac{x}{x+\kappa}$ is bounded by $\frac{1}{\kappa}$.

Then using equation (31) and definition (46) of v, we find the following estimate for all $x \ge \frac{\varepsilon}{2}$:

$$\begin{aligned}|\partial_t F^\varepsilon(t,x) + v\partial_x F^\varepsilon(t,x)| \le{}& 2\|a'\|_\infty\int_{x-\varepsilon}^{x} f^\varepsilon(t,y)\mathrm{d}y + \frac{1}{\varepsilon}\frac{a(x)}{\kappa}|L^\varepsilon(t) - L(t)|\int_{x-\varepsilon}^{x} f^\varepsilon(t,y)\mathrm{d}y\\ &+ 2\|b'\|_\infty\int_{x}^{x+\varepsilon} f^\varepsilon(t,y)\mathrm{d}y\\ &+ a(x)\frac{L(t)}{L(t)+\kappa}|\partial_x F^\varepsilon(t,x) - \Delta_{-\varepsilon}F^\varepsilon(t,x)|\\ &+ b(x)|\partial_x F^\varepsilon(t,x) - \Delta_\varepsilon F^\varepsilon(t,x)|.\end{aligned}$$

Now, for all $x < \frac{\varepsilon}{2}$, using equation (32), assumption (H'1) and since $\partial_x F^\varepsilon(t,x) = -f^\varepsilon(t,x)$, we find:

$$\begin{aligned}
&|\partial_t F^\varepsilon(t,x) + v\partial_x F^\varepsilon(t,x)| \\
&\quad \le |\frac{1}{\varepsilon}\int_{-\frac{\varepsilon}{2}}^{x} a^\varepsilon(y)\frac{L^\varepsilon(t)}{L^\varepsilon(t)+\kappa} f^\varepsilon(t,y)\mathrm{d}y - a(x)\frac{L(t)}{L(t)+\kappa} f^\varepsilon(t,x)| \\
&\qquad + |\frac{1}{\varepsilon}\int_{\frac{\varepsilon}{2}}^{x+\varepsilon} b^\varepsilon(y) f^\varepsilon(t,y)\mathrm{d}y - b(x) f^\varepsilon(t,x)|.
\end{aligned}$$

The term involving a and a^ε is bounded by adding and removing the appropriate terms and observing that for all $x < \varepsilon/2$, $f^\varepsilon(t,x) = c_0^\varepsilon(t)$:

$$\begin{aligned}
&|\frac{1}{\varepsilon}\int_{-\frac{\varepsilon}{2}}^{x} a^\varepsilon(y)\frac{L^\varepsilon(t)}{L^\varepsilon(t)+\kappa} f^\varepsilon(t,y)\mathrm{d}y - a(x)\frac{L(t)}{L(t)+\kappa} f^\varepsilon(t,x)| \\
&\qquad \le |\frac{x+\frac{\varepsilon}{2}}{\varepsilon}a(0)\frac{L^\varepsilon(t)}{L^\varepsilon(t)+\kappa}c_0^\varepsilon(t) - a(x)\frac{L(t)}{L(t)+\kappa}c_0^\varepsilon(t)| \\
&\qquad \le a(0)c_0^\varepsilon(t)\frac{x+\frac{\varepsilon}{2}}{\varepsilon}|\frac{L^\varepsilon(t)}{L^\varepsilon(t)+\kappa} \\
&\qquad\quad - \frac{L(t)}{L(t)+\kappa}| + |a(x) - \frac{x+\frac{\varepsilon}{2}}{\varepsilon}a(0)|\frac{L^\varepsilon(t)}{L^\varepsilon(t)+\kappa}c_0^\varepsilon(t) \\
&\qquad \le \frac{a(0)c_0^\varepsilon(t)}{\kappa}\frac{x+\frac{\varepsilon}{2}}{\varepsilon}|L^\varepsilon(t) - L(t)| + \left(|a(x)-a(0)| + a(0)\frac{\frac{\varepsilon}{2}-x}{\varepsilon}\right)c_0^\varepsilon(t) \\
&\qquad \le \frac{a(0)c_0^\varepsilon(t)}{\kappa}|L^\varepsilon(t) - L(t)| + (\frac{\varepsilon}{2}\|a'\|_\infty + a(0))c_0^\varepsilon(t).
\end{aligned}$$

In the right hand side of the last inequality, the first term is bounded using Lemma 3.2 as well as the term involving $\|a'\|_\infty$. The remaining term $a(0)c_0^\varepsilon(t)$ is bounded using Lemma 3.3, hence there exists a positive constant C independent of ε such that for ε small enough and for all $t \in (0,T]$, $a(0)c_0^\varepsilon(t) \le \varepsilon(c_0^{\varepsilon,0} + C)$ and since we assume assumption (H9) to hold true, we finally obtain for all $x \le \frac{\varepsilon}{2}$:

$$\begin{aligned}
&|\frac{1}{\varepsilon}\int_{-\frac{\varepsilon}{2}}^{x} a^\varepsilon(y)\frac{L^\varepsilon(t)}{L^\varepsilon(t)+\kappa} f^\varepsilon(t,y)\mathrm{d}y - a(x)\frac{L(t)}{L(t)+\kappa} f^\varepsilon(t,x)| \\
&\quad \le \frac{a(0)\bar{c_0}}{\kappa}|L^\varepsilon(t) - L(t)| + \varepsilon\left(K + C + \frac{\|a'\|_\infty \bar{c_0}}{2}\right).
\end{aligned}$$

The term in b and b^ε is easily bounded using assumption (H2b) and Lemma 3.2:

$$\begin{aligned}
&|\frac{1}{\varepsilon}\int_{\frac{\varepsilon}{2}}^{x+\varepsilon} b^\varepsilon(y) f^\varepsilon(t,y)\mathrm{d}y - b(x) f^\varepsilon(t,x)| \\
&= |\frac{x+\frac{\varepsilon}{2}}{\varepsilon}b_1^\varepsilon c_1^\varepsilon(t) - b(x)c_0^\varepsilon(t)| \le C_b\varepsilon\left(\bar{c_1} + \frac{\bar{c_0}}{2}\right)
\end{aligned}$$

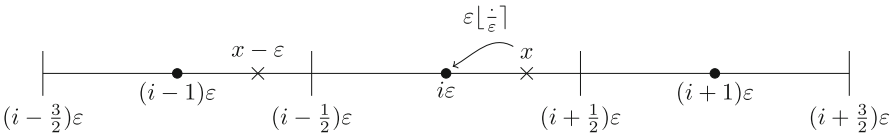

Fig. 2 Representation of the cells Γ^ε_{i-1}, Γ^ε_i and Γ^ε_{i+1} and of the value $\varepsilon\lfloor\frac{x}{\varepsilon}\rceil$

Now we can integrate $|\partial_t F^\varepsilon(t,\cdot) + v\partial_x F^\varepsilon(t,\cdot)|$ over $\mathbb{R}_+$ using the two previous estimates. Note that using Fubini's theorem and Eq. (33), we have

$$\begin{aligned}
&\int_{\frac{\varepsilon}{2}}^{+\infty}\int_{x-\varepsilon}^{x} f^\varepsilon(t,y)\mathrm{d}y\mathrm{d}x \\
&= \int_{-\frac{\varepsilon}{2}}^{+\infty} f^\varepsilon(t,y)\int_{\max(y,\varepsilon/2)}^{y+\varepsilon}\mathrm{d}x\mathrm{d}y \\
&= \int_{-\frac{\varepsilon}{2}}^{\frac{\varepsilon}{2}} f^\varepsilon(t,y)\int_{\frac{\varepsilon}{2}}^{y+\varepsilon}\mathrm{d}x\mathrm{d}y + \int_{\frac{\varepsilon}{2}}^{+\infty} f^\varepsilon(t,y)\int_{y}^{y+\varepsilon}\mathrm{d}x\mathrm{d}y \\
&= c_0^\varepsilon(t)\int_{-\frac{\varepsilon}{2}}^{\frac{\varepsilon}{2}}(y+\frac{\varepsilon}{2})\mathrm{d}y + \varepsilon\int_{\frac{\varepsilon}{2}}^{+\infty} f^\varepsilon(t,y)\mathrm{d}y \\
&= \frac{\varepsilon^2}{2}c_0^\varepsilon(t) + \varepsilon\int_{\frac{\varepsilon}{2}}^{+\infty} f^\varepsilon(t,y)\mathrm{d}y = \varepsilon\int_0^{\frac{\varepsilon}{2}} f^\varepsilon(t,y)\mathrm{d}y + \varepsilon\int_{\frac{\varepsilon}{2}}^{+\infty} f^\varepsilon(t,y)\mathrm{d}y \\
&= \varepsilon\int_0^{+\infty} f^\varepsilon(t,y)\mathrm{d}y \le \varepsilon m.
\end{aligned}$$

Therefore, we get:

$$\begin{aligned}
\int_{\mathbb{R}_+}|\partial_t F^\varepsilon(t,x) + v\partial_x F^\varepsilon(t,x)|\mathrm{d}x &\le \varepsilon(2\|a'\|_\infty + 2\|b'\|_\infty|)m \\
&+ \frac{\|a\|_\infty}{\kappa}|L^\varepsilon(t) - L(t)|m \\
&+ \|a\|_\infty\frac{L(t)}{L(t)+\kappa}\int_{\frac{\varepsilon}{2}}^{+\infty}|\partial_x F^\varepsilon(t,x) - \Delta_{-\varepsilon}F^\varepsilon(t,x)|\mathrm{d}x \\
&+ \int_{\frac{\varepsilon}{2}}^{+\infty} b(x)|\partial_x F^\varepsilon(t,x) - \Delta_\varepsilon F^\varepsilon(t,x)|\mathrm{d}x \\
&+ \frac{a(0)\bar{c_0}}{\kappa}|L^\varepsilon(t) - L(t)| + \varepsilon(K + C + \frac{\|a'\|_\infty\bar{c_0}}{2}) + C_b\varepsilon\left(\bar{c_1} + \frac{\bar{c_0}}{2}\right).
\end{aligned} \tag{39}$$

We now compute the difference between the continuous and discrete derivatives on F^ε. We denote by $\lfloor x\rceil$ the nearest integer function with the upper-rounding convention: $\lfloor 0.5\rceil = 1$. Figure 2 shows a representation of the cells Γ^ε_{i-1}, Γ^ε_i and Γ^ε_{i+1} as well as an example of the result of $\lfloor\frac{x}{\varepsilon}\rceil$ for $x \in \Gamma^\varepsilon_i$.

Let us first compute the integral of $|\partial_x F^\varepsilon(t,x) - \Delta_{-\varepsilon} F^\varepsilon(t,x)|$, using Eq. (36) and the fact that f^ε is constant equal to $c_i^\varepsilon(t)$ on the cells Γ_i^ε:

$$\begin{aligned}
&\int_{\frac{\varepsilon}{2}}^{+\infty} |\partial_x F^\varepsilon(t,x) - \Delta_{-\varepsilon} F^\varepsilon(t,x)| \mathrm{d}x \\
&\quad = \int_{\frac{\varepsilon}{2}}^{+\infty} |f^\varepsilon(t,x) - \frac{1}{\varepsilon}\int_{x-\varepsilon}^{x} f^\varepsilon(t,y)\mathrm{d}y| \mathrm{d}x \\
&= \int_{\frac{\varepsilon}{2}}^{+\infty} \frac{1}{\varepsilon} |\int_{x-\varepsilon}^{x} (f^\varepsilon(t,x) - f^\varepsilon(t,y))\mathrm{d}y| \mathrm{d}x \\
&= \int_{\frac{\varepsilon}{2}}^{+\infty} \frac{1}{\varepsilon} |\int_{x-\varepsilon}^{\varepsilon(\lfloor \frac{x}{\varepsilon} \rceil - \frac{1}{2})} (f^\varepsilon(t,x) - f^\varepsilon(t,y))\mathrm{d}y| \mathrm{d}x \\
&= \int_{\frac{\varepsilon}{2}}^{+\infty} |c^\varepsilon_{\lfloor \frac{x}{\varepsilon} \rceil}(t) - c^\varepsilon_{\lfloor \frac{x}{\varepsilon} \rceil - 1}(t)| \frac{\varepsilon(\lfloor \frac{x}{\varepsilon} \rceil - \frac{1}{2}) - (x-\varepsilon)}{\varepsilon} \mathrm{d}x.
\end{aligned}$$

Now, observe that for all $x \in \Gamma_i^\varepsilon$ one has $c^\varepsilon_{\lfloor \frac{x}{\varepsilon} \rceil}(t) - c^\varepsilon_{\lfloor \frac{x}{\varepsilon} \rceil - 1}(t) = c_i^\varepsilon(t) - c_{i-1}^\varepsilon(t)$, which gives:

$$\begin{aligned}
\int_{\frac{\varepsilon}{2}}^{+\infty} |\partial_x F^\varepsilon(t,x) - \Delta_{-\varepsilon} F^\varepsilon(t,x)| \mathrm{d}x &= \sum_{i \geq 1} |c_i^\varepsilon(t) - c_{i-1}^\varepsilon(t)| \int_{\Gamma_i^\varepsilon} \frac{\varepsilon(\lfloor \frac{x}{\varepsilon} \rceil - \frac{1}{2}) - (x-\varepsilon)}{\varepsilon} \mathrm{d}x \\
&= \frac{\varepsilon}{2} \sum_{i \geq 1} |c_i^\varepsilon(t) - c_{i-1}^\varepsilon(t)|.
\end{aligned}$$

Hence, according to Lemma 3.4 there exists a constant $C(T) > 0$ independent of ε such that:

$$\int_{\frac{\varepsilon}{2}}^{+\infty} |\partial_x F^\varepsilon(t,x) - \Delta_{-\varepsilon} F^\varepsilon(t,x)| \mathrm{d}x \leq \varepsilon C(T). \tag{40}$$

We proceed similarly for the term $\int_{\mathbb{R}_+} b(x) |\partial_x F^\varepsilon(t,x) - \Delta_\varepsilon F^\varepsilon(t,x)| \mathrm{d}x$:

$$\begin{aligned}
&\int_{\frac{\varepsilon}{2}}^{\infty} b(x) |f^\varepsilon(t,x) - \frac{1}{\varepsilon}\int_{x}^{x+\varepsilon} f^\varepsilon(t,y)\mathrm{d}y| \mathrm{d}x \\
&\quad = \int_{\frac{\varepsilon}{2}}^{\infty} \frac{b(x)}{\varepsilon} |\int_{x}^{x+\varepsilon} (f^\varepsilon(t,x) - f^\varepsilon(t,y))\mathrm{d}y| \mathrm{d}x \\
&\quad = \int_{\frac{\varepsilon}{2}}^{\infty} \frac{b(x)}{\varepsilon} |\int_{\varepsilon(\lfloor \frac{x}{\varepsilon} \rceil + \frac{1}{2})}^{x+\varepsilon} (f^\varepsilon(t,x) - f^\varepsilon(t,y))\mathrm{d}y| \mathrm{d}x \\
&\quad = \int_{\frac{\varepsilon}{2}}^{\infty} |c^\varepsilon_{\lfloor \frac{x}{\varepsilon} \rceil + 1}(t) - c^\varepsilon_{\lfloor \frac{x}{\varepsilon} \rceil}(t)| b(x) \frac{x - \varepsilon(\lfloor \frac{x}{\varepsilon} \rceil - \frac{1}{2})}{\varepsilon} \mathrm{d}x
\end{aligned}$$

$$= \sum_{i\geq 1} |c_{i+1}^{\varepsilon}(t) - c_i^{\varepsilon}(t)| \int_{\Gamma_i^{\varepsilon}} b(x) \frac{x - \varepsilon(\lfloor \frac{x}{\varepsilon} \rceil - \frac{1}{2})}{\varepsilon} \mathrm{d}x.$$

Owing to hypothesis (H2b), we simply bound the last integral as follows:

$$\int_{\Gamma_i^{\varepsilon}} b(x) \frac{x - \varepsilon(\lfloor \frac{x}{\varepsilon} \rceil - \frac{1}{2})}{\varepsilon} \mathrm{d}x \leq C_b \frac{\varepsilon^2}{2}(i + \frac{1}{6}).$$

Hence, according to Lemma 3.4, there exists a constant $C(T) > 0$ independent of ε such that:

$$\int_{\frac{\varepsilon}{2}}^{+\infty} b(x) |\partial_x F^{\varepsilon}(t,x) - \Delta_x F^{\varepsilon}(t,x)| \mathrm{d}x < \frac{\varepsilon}{6} C(T)(1 + \frac{\varepsilon}{2}). \tag{41}$$

We conclude from Eqs. (39)–(40)–(41) by regrouping together terms not depending on ε.

□

We now proceed with the proof of Theorem 3.1.

Proof of Theorem 3.1 Let $T > 0$ and consider $t \in (0, T]$. We begin by integrating (37) over $[0, t]$, using Lemma 3.7:

$$\begin{aligned}
\int_{\mathbb{R}_+} |E(t,x)| \mathrm{d}x &\leq \int_{\mathbb{R}_+} |E(0,x)| \mathrm{d}x + (\|a'\|_{\infty} + \|b'\|_{\infty}) \int_0^t \int_{\mathbb{R}_+} |E(s,x)| \mathrm{d}x \mathrm{d}s \\
&\quad + \int_0^t \int_{\mathbb{R}_+} |\partial_t F^{\varepsilon}(s,x) + v(x, L(s)) \partial_x F^{\varepsilon}(s,x)| \mathrm{d}x \mathrm{d}s + \frac{\varepsilon}{2} a(0) T \bar{c_0} \\
&\leq \int_{\mathbb{R}_+} |E(0,x)| \mathrm{d}x + (\|a'\|_{\infty} + \|b'\|_{\infty}) \int_0^t \int_{\mathbb{R}_+} |E(s,x)| \mathrm{d}x \mathrm{d}s \\
&\quad + \varepsilon T C_1 + C_2 \int_0^t |L^{\varepsilon}(s) - L(s)| \mathrm{d}s + \frac{\varepsilon}{2} a(0) T \bar{c_0}.
\end{aligned}$$

Then observe that:

$$\int_{\mathbb{R}_+} x f^{\varepsilon}(t,x) dx = \int_{\mathbb{R}_+} x \sum_{i\geq 0} \mathbb{1}_{\Gamma_i^{\varepsilon}}(x) c_i^{\varepsilon}(t) \mathrm{d}x = \sum_{i\geq 0} \int_{\Gamma_i^{\varepsilon}} x \mathrm{d}x c_i^{\varepsilon}(t) = \sum_{i\geq 0} i\varepsilon^2 c_i^{\varepsilon}(t).$$

Using conservation equations (14c) and (7) and Fubini's theorem, this leads to the bound:

$$\begin{aligned}
|L^{\varepsilon}(t) - L(t)| &= |\int_0^{\infty} x(f^{\varepsilon}(t,x) - f(t,x)) \mathrm{d}x| \\
&= |\int_0^{\infty} (F^{\varepsilon}(t,x) - F(t,x)) \mathrm{d}x| \leq \int_{\mathbb{R}_+} |E(t,x)| \mathrm{d}x,
\end{aligned}$$

which finally yields:

$$
\begin{aligned}
&|L^\varepsilon(t) - L(t)| + \int_{\mathbb{R}_+} |E(t,x)|\mathrm{d}x \\
&\quad \le 2\int_{\mathbb{R}_+} |E(0,x)|\mathrm{d}x + 2(\|a'\|_\infty + \|b'\|_\infty) \\
&\quad \int_0^t \int_{\mathbb{R}_+} |E(s,x)|\mathrm{d}x\mathrm{d}s \\
&\quad + 2\varepsilon T C_1 + 2C_2 \int_0^t |L^\varepsilon(s) - L(s)|\mathrm{d}s + \varepsilon a(0) T \bar{c_0}.
\end{aligned}
$$

By the assumption on $E(0,x)$ and Grönwall's lemma, we finally conclude that:

$$
\begin{aligned}
&|L^\varepsilon(t) - L(t)| + \int_{\mathbb{R}_+} |E(t,x)|\mathrm{d}x \\
&\quad \le \varepsilon\Big(2C_{\text{init}} + 2C_1 T + a(0) T \bar{c_0}\Big) \\
&\quad \exp(2(\|a'\|_\infty + \|b'\|_\infty + C_2)T).
\end{aligned}
$$

□

4 Derivation of second order model and stationary solutions

4.1 A second-order Lifshitz–Slyozov model with diffusion

Up to this point we have studied a Lifshitz–Slyozov model, that is to say a transport PDE. However, this model leads to stationary solutions which are combinations of Dirac masses centered at the zeros of velocity v. Hence, since we aim at obtaining asymptotically bimodal distributions, we would like to add a diffusion term to our model in order to smooth the stationary solutions. Unfortunately and up to our knowledge, no biological argument can be found to explain such a diffusive term or to give a proper way of deriving it from biological considerations. Nonetheless, one can see this diffusive term as a second order term emerging from the preceding convergence result, see for example (Vasseur et al. 2002; Schlichting 2019; Deschamps et al. 2017). We expect the asymptotic solutions to Lifshitz–Slyozov model with diffusion to approximate better the solutions to Becker–Döring system, when ε is small. However, we are not able to provide convergence results in the large time limit.

We follow here the derivation of the diffusive term presented in Vasseur et al. (2002) and we use the notation introduced at Sect. 3.

Now, from Proposition 2.2, we can add and subtract the appropriate terms in ϕ to get:

$$\begin{aligned}
&\int_0^\infty (f^\varepsilon(t,x) - f^\varepsilon(0,x))\phi(x)\mathrm{d}x \\
&= \int_0^t \int_0^\infty (\Delta_\varepsilon \phi(x) a^\varepsilon(x) \frac{L^\varepsilon(t)}{L^\varepsilon(t)+\kappa} - \Delta_{-\varepsilon}\phi(x) b^\varepsilon(x)) f^\varepsilon(t,x)\mathrm{d}x\mathrm{d}t \\
&= \int_0^t \int_0^\infty \frac{\phi(x+\varepsilon)-\phi(x-\varepsilon)}{2\varepsilon}(a^\varepsilon(x)\frac{L^\varepsilon(t)}{L^\varepsilon(t)+\kappa} - b^\varepsilon(x)) f^\varepsilon(t,x)\mathrm{d}x\mathrm{d}t \\
&\quad + \frac{\varepsilon}{2}\int_0^t \int_0^\infty \frac{\phi(x+\varepsilon)-2\phi(x)+\phi(x-\varepsilon)}{\varepsilon^2} a^\varepsilon(x)\frac{L^\varepsilon(t)}{L^\varepsilon(t)+\kappa} f^\varepsilon(t,x)\mathrm{d}x\mathrm{d}t \\
&\quad + \frac{\varepsilon}{2}\int_0^t \int_0^\infty \frac{\phi(x+\varepsilon)-2\phi(x)+\phi(x-\varepsilon)}{\varepsilon^2} b^\varepsilon(x) f^\varepsilon(t,x)\mathrm{d}x\mathrm{d}t \\
&= \int_0^t \int_0^\infty \bar{\Delta}_\varepsilon \phi(x)(a^\varepsilon(x)\frac{L^\varepsilon(t)}{L^\varepsilon(t)+\kappa} - b^\varepsilon(x)) f^\varepsilon(t,x)\mathrm{d}x\mathrm{d}t \\
&\quad + \frac{\varepsilon}{2}\int_0^t \int_0^\infty \Delta_\varepsilon^2 \phi(x)(a^\varepsilon(x)\frac{L^\varepsilon(t)}{L^\varepsilon(t)+\kappa} + b^\varepsilon(x)) f^\varepsilon(t,x)\mathrm{d}x\mathrm{d}t
\end{aligned}$$

where $\bar{\Delta}_h\phi(x) = \frac{\phi(x+h)-\phi(x-h)}{2h}$ and $\Delta_h^2\phi(x) = \frac{\phi(x+h)-2\phi(x)+\phi(x-h)}{h^2}$.

This leads us to study the PDE (18).

4.2 Stationary solutions for the second-order Lifshitz–Slyozov model

In this section, we present the stationary solutions of system (11) without diffusion and system (18) with diffusion. The stationary solutions of system (18) have previously been described in Hariz and Collet (1999); Vasseur et al. (2002); Goudon and Monasse (2020). We notice that stationary solutions are very different in nature from one model to the other. Equation(11) does not yield nontrivial smooth stationary functions, and we rather expect stationary solutions to be linear combinations of Dirac masses, located at roots of the asymptotic velocity.

We can compute explicitly stationary solutions of system (18), namely:

$$\partial_t g = 0 \Longleftrightarrow \partial_x(vg) - \frac{\varepsilon}{2}\partial_x^2(dg) = 0.$$

Together with boundary conditions (17) this leads to stationary solutions denoted by $M_{L_{\text{stat}}}$, depending on stationary $L_{\text{stat}} \in \mathbb{R}_+$ under the form:

$$M_{L_{\text{stat}}}(x) = \frac{C(m, L_{\text{stat}})}{d(x, L_{\text{stat}})} \exp\left(\frac{2}{\varepsilon}\int_0^x \frac{v(y, L_{\text{stat}})}{d(y, L_{\text{stat}})}\mathrm{d}y\right), \tag{42}$$

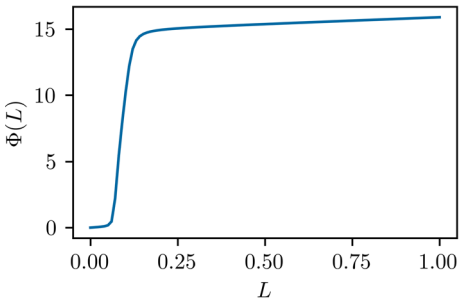

Fig. 3 Plot of function $L \to \Phi(L)$ for $L \in [10^{-12}, 1]$ with functions a and b defined at Eqs. (4) and (5) and parameters given at Table 1

where the constant $C(m, L_{\text{stat}})$ is determined in order to satisfy $\int_{\mathbb{R}_+} M_{L_{\text{stat}}}(t, x)\mathrm{d}x = m$, that is to say

$$C(m, L_{\text{stat}}) = \frac{m}{\displaystyle\int_{\mathbb{R}_+} \frac{1}{d(x, L_{\text{stat}})} \exp\Big(\frac{2}{\varepsilon}\int_0^x \frac{v(y, L_{\text{stat}})}{d(y, L_{\text{stat}})}\mathrm{d}y\Big)\mathrm{d}x}$$

and L_{stat} solves the constraint equation

$$L_{\text{stat}} + \int_{\mathbb{R}_+} x M_{L_{\text{stat}}}(x)\mathrm{d}x = \lambda. \tag{43}$$

Note that function $\Phi : L \to L + \displaystyle\int_{\mathbb{R}_+} x M_L(x)\mathrm{d}x$ is continuous on $\mathbb{R}_+$. Moreover, straightforward computations show that thanks to expression (42) and expressions for a and b that $\Phi(0) = 0$ and $\Phi \underset{L\to+\infty}{\to} +\infty$. Therefore, for all $\lambda \geq 0$, there exists at least one value for L which satisfies Eq. (43). Regarding unicity of stationary solutions, it would need to prove strict monotonicity of Φ, which is so far an open question. However, we may observe numerically that the application $\Phi : L \to L + \int_0^{x_{\max}} x M_L(x)\mathrm{d}x$ seems strictly non-decreasing, see Fig. 3.

Remark In other modeling contexts, one may choose different functions a and b such that existence of stationary solutions may not be true for all value of λ. For example, $a(x) = 1$ and $b(x) = x^s$ with $s \leq 1$ implies $\lim_{L\to 0^+} \Phi(L) = \lambda_0 > 0$. Hence for values of λ such that $\lambda < \lambda_0$, the system might not have smooth stationary solutions, see Sect. 5.2.5 and Figs. 13 and 14.

In the following section, we will present some numerical simulations for system (18) and control that stationary solutions $M_{L_{\text{stat}}}$ follow a bimodal distribution for well-chosen parameters.

5 Numerical simulations

In this part, we use a finite volume well-balanced scheme introduced in Goudon and Monasse (2020) to approximate time dependent solutions to Eq. (18). This scheme is inspired by the work in Jin and Yan (2011). Afterwards, we explore numerically the solutions to system (18) for various sets of parameters. We also compare the Lifshitz–Slyozov diffusive equation with the transport equation (11) and with the transport equation (11) with a constant diffusive term. We will finally explore the case when $\lambda < \lambda_0 = \lim_{L\to 0^+} \Phi(L) => 0$ mentioned previously in the remark of Sec. 4.2.

Note that in this section, unlike the previous ones, we are working on a bounded domain $x \in [0, x_{\max}]$ rather than on $\mathbb{R}^+$.

5.1 A well-balanced numerical scheme for system (18)

In the following, we will need to compute some approximations for the stationary solutions $M_{L_{\text{stat}}}$ since we need them in the well-balanced scheme, see later on. Moreover, it will enable us to compare the asymptotic profiles with the stationary solutions in the numerical tests.

Let us recall that stationary solutions $M_{L_{\text{stat}}}$ are defined by an explicit expression given at Eq. (42) with L_{stat} satisfying constraint equation (43). Therefore, to compute this stationary solution, a simple dichotomy method is implemented to find the solution to $\Phi(L) = \lambda$, since the application Φ is increasing in the range of L that interests us, see Fig. 3. We use the trapezoidal rule for the computation of the integrals.

Since we are interested in a conservative PDE, we use a finite volume scheme. We also aim at capturing correctly stationary solutions and for that purpose, we implement a well-balanced scheme introduced in Goudon and Monasse (2020). Let us detail the scheme here.

The scheme is based on a change of variables in the PDE (18) to obtain a symmetric operator. This will allow simpler calculations down the line. Denote D_L the spatial operator in the PDE, i.e.:

$$D_L g = \partial_x F(g; x, L) = \partial_x \Big(- v(x, L) g + \partial_x (d(x, L) g) \Big).$$

We recall that the stationary solution associated with the value L is given by:

$$M_L(x) = \frac{C(m, L)}{d(x, L)} \exp\Big(\int_0^x \frac{v(y, L)}{d(y, L)} \mathrm{d}y \Big). \tag{44}$$

This stationary solution satisfies $D_L M_L = 0$ and we can rewrite the operator D_L in the following way:

$$D_L g = \partial_x \Big(d(x, L) M_L \partial_x (\frac{g}{M_L}) \Big).$$

Then we perform the change of variable $h = \frac{g}{\sqrt{M_L}}$ and introduce the new operator $\tilde{D}_L$, which is symmetric for the L^2 inner product:

$$\tilde{D}_L h = \frac{1}{\sqrt{M_L}} D_L(h\sqrt{M_L}) = \frac{1}{\sqrt{M_L}} \partial_x \Big(d(x, L) M_L \partial_x (\frac{h}{\sqrt{M_L}}) \Big).$$

Note that we use an implicit discretization in time in order to avoid a constraining time step for the diffusion operator.

Given a mesh of size $\Delta x > 0$ in space, we discretize the interval $[0, x_{\max}]$ and consider N cells $\mathcal{C}_j = [x_{j-1/2}, x_{j+1/2}]$, $1 \leq j \leq N$ centered at point x_j, with $x_j = j\Delta x$ and $x_{j+1/2} = (j + 1/2)\Delta x$. We also introduce a time step $\Delta t > 0$ and the discretization times $t_n = n\Delta t$, $n \in \mathbb{N}$.

We denote by h_j^n an approximation of the average of function h on cell $\mathcal{C}_j$ at time t_n, that is to say $h_j^n \sim \frac{1}{\Delta x} \int_{\mathcal{C}_j} h(t_n, x) \mathrm{d}x$. We also define $M_{L^n,j}$ as an approximation of stationary solution M_{L^n} defined at Eq. (44) at point x_j with $L = L^n$, and $D_{j+1/2}^n$ as an approximation of diffusion coefficient $d(x_{j+1/2}, L^n)$ at point $x_{j+1/2}$ with $L = L^n$, see expression (16).

We denote by $F_{j+1/2}^n$ an approximation of flux $d(x, L) M_L \partial_x (\frac{h}{\sqrt{M_L}})$ at the boundary $x_{j+1/2}$ of cell $\mathcal{C}_j$ at time t_n.

We therefore discretize Eq. (18a) as follows:

$$\begin{aligned}
\frac{h_{j+1}^n - h_j^n}{\Delta t} &= \frac{1}{\Delta x \sqrt{M_{L^n,j}}} (F_{j+1/2}^n - F_{j-1/2}^n) \\
&= \frac{1}{\Delta x \sqrt{M_{L^n,j}}} \Big(D_{j+1/2}^n \sqrt{M_{L^n,j+1} M_{L^n,j}} \frac{h_{j+1}^{n+1}/\sqrt{M_{L^n,j+1}} - h_j^{n+1}/\sqrt{M_{L^n,j}}}{\Delta x} \\
&\quad - D_{j-1/2}^n \sqrt{M_{L^n,j} M_{L^n,j-1}} \frac{h_j^{n+1}/\sqrt{M_{L^n,j}} - h_{j-1}^{n+1}/\sqrt{M_{L^n,j-1}}}{\Delta x} \Big).
\end{aligned}$$

Regarding boundary conditions, we want to preserve the zeroth-order moment $\int_0^{x_{\max}} g(t, x) \mathrm{d}x = \int_0^{x_{\max}} g^0(x) \mathrm{d}x$, which implies to use the following null-flux boundary conditions:

$$-v(x, L(t)) g(t, x) + \frac{\varepsilon}{2} \partial_x (d(x, L(t)) g(t, x))|_{x=0, x_{\max}} = 0.$$

The boundary conditions are implemented by using the null-flux conditions for the flux computed at $x_{-1/2}$ and $x_{N+1/2}$. This amounts to setting $F_{-1/2}^n = F_{N+1/2}^n = 0$ in the text.

In order to update the value of L, we derive Eq. (18b) with respect to time and we discretize the equation $\partial_t L = -\int_{\mathbb{R}_+} x\,\partial_t g(t,x)\mathrm{d}x$, which gives:

$$L^{n+1} = L^n - \Delta x \sum_{i=1}^{N} x_i (g_i^{n+1} - g_i^n).$$

This update leads to a restriction on the time step Δt to preserve positivity of L^{n+1} as seen in Goudon and Monasse (2020). Then a sufficient condition would be to set :

$$\Delta t |P^{-1} B^n| |P g^n| \leq L^n.$$

where B^n is defined as:

$$B_i^n = \begin{cases} -D_{1/2}^n \dfrac{M_{L^n,1/2}}{M_{L^n,0}}, & \text{if } i = 0, \\ \dfrac{1}{M_{L^n,i}} (D_{L^n,i+1/2} M_{L^n,i+1/2} - D_{i-1/2}^n M_{L^n,i-1/2}), & \text{otherwise.} \end{cases}$$

5.2 Numerical results

The previous numerical scheme enables us to explore the properties of system (18) as a model for adipocyte distribution evolution in time. Table 1 presents the value of most parameters for the simulations. Unless stated otherwise, these parameters shall be fixed for this section. Concerning values of parameters, a few of them are chosen in accordance with biological observations. V_{lipids} and r_0 have fixed given values. The value of γ is taken from Soula et al. (2015). Values of other parameters are chosen as to observe bimodal distributions. We refer the reader to Giacobbi et al. (2023) for further investigation into the values of those parameters.

5.2.1 Asymptotic behaviour of the second order Lifshitz–Slyozov system (18)

To begin with, we check that the asymptotic profile obtained with the time evolution of the solution thanks to the previous described scheme coincides with the stationary solution of Sec. 4.2.

First, one may assume that given an initial condition (g^0, L^0), the asymptotic behaviour of the system is governed by the two parameters m and λ. This means that given two initial conditions (g_1^0, L_1^0) and (g_2^0, L_2^0) such that $m_1 = m_2$ and $\lambda_1 = \lambda_2$, the stationary solutions are equal. In Fig. 4b, both initial conditions are Gaussian functions centered at $x_1 = 1$ and $x_2 = 3$ with $m_1 = m_2$ and initial values L_1^0 and L_2^0 are chosen so that $\lambda_1 = \lambda_2$. We indeed observe that the asymptotic profile is the same for these two initial conditions. From numerical explorations, we believe that this is a general behaviour of the model. For different boundary conditions, a proof of the

Table 1 Values of parameters for the model

Parameter	Value	Unit	Description	Related equation
α	0.7	nmol h^{-1} μm^{-1}	Lipogenesis surface limited flow rate	Eq. (4)
ρ	200	μm	Lipogenesis saturation in radius cutoff	Eq. (4)
n	3	Ø	Lipogenesis saturation in radius power	Eq. (4)
κ	0.01	Ø	Lipogenesis saturation in external lipid constant	Eq. (4)
β	1	nmol h^{-1}	Lipolysis basal flow rate	Eq. (5)
γ	0.27	nmol h^{-1} μm^{-1}	Lipolysis surface limited flow rate	Eq. (5)
χ	0.01	Ø	Lipolysis saturation in internal lipid constant	Eq. (5)
V_{lipids}	10^6	μm^3	Molar volume of triglycerides	Eq. (1)
r_0	6	μm	Radius of an adipocyte without lipid	Eq. (1)
ε	0.05	Ø	Diffusion scaling parameter	Eq. (18a)
$x_{\max}$	15	nmol	Maximal lipid size of an adipocyte	Sec. 5.1
N	10^4	Ø	Number of discretization points	Sec. 5.1

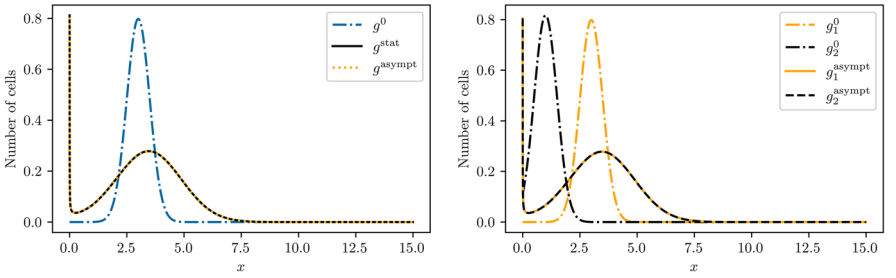

(a) Comparison with stationary solution and asymptotic profile of the numerical scheme.

(b) Comparison of two asymptotic profiles from two different initial conditions.

Fig. 4 Left : Distributions of adipocytes with respect to size, i.e. amount of lipids, starting with $\lambda = 3.5$ and initial distribution $g^0(x) = C \exp\left(-\frac{1}{2}\left(\frac{x-3}{0.5}\right)^2\right)$ (in dashed blue line): asymptotic profile (dotted yellow line) and stationary solution (black full line) both present bimodality. Parameters of the system are given at Table 1. Right : Asymptotic profiles g_1^{asympt} and g_2^{asympt}, from two initial conditions (g_1^0, L_1^0) and (g_2^0, L_2^0) such that $m_1 = m_2$ and $\lambda_1 = \lambda_2$. Note that the two asymptotic distributions are superimposed

uniqueness of stationary solutions can be found in Hariz and Collet (1999). We are unaware of a proof that would work in our case, but we think that the result should also hold true. Moreover, up to our knowledge, no proof of the asymptotic behaviour of the diffusive Lifshitz–Slyozov system is available for the moment, see Conlon and Schlichting (2019) on a related but different equation.

5.2.2 Bimodality vs unimodality

Since the main aim of the model we develop and study in this paper is to represent bimodality of the distribution on the stationary solution, we check if we effectively find some parameter ranges for which we observe this behaviour. In particular, we investigate the dependency with respect to λ. Note that, since λ is defined by expression (7), we change λ by changing the initial conditions L^0 and g^0, in the case of time evolution of the system, or by changing the value of L^{stat} when considering stationary solutions.

In Fig. 4a, we plot densities of adipocytes as a function of size x. It shows the result of the scheme starting from a Gaussian initial condition $g^0(x) = C \exp\left(-\frac{1}{2}\left(\frac{x-3}{0.5}\right)^2\right)$ plotted in dashed blue line and L^0 such that $\lambda = 3.5$. The value of C is determined such that $m = 1$. The stationary solution is denoted $g^{\text{stat}} = M_{L_{\text{stat}}}$ - in black full line - and the final result of the scheme at time $t = t_{\max}$ is denoted $g(t_{\max}, \cdot)$ and represented in dotted yellow line. $t_{\max}$ is determined such that the relative difference between the size distribution $g(t_{\max}, \cdot)$ and the stationary solution $M_{L_{\text{stat}}}$ is less than 5×10^{-5}. We can observe that bimodality is obtained for the stationary solution as well as for the asymptotic profile of the adipocyte size distribution and that there is a good correspondence between the two functions. Up to some numerical error of order 10^{-12}, both the initial number of cells $m = \int_0^{x_{\max}} g^0(x)\mathrm{d}x$

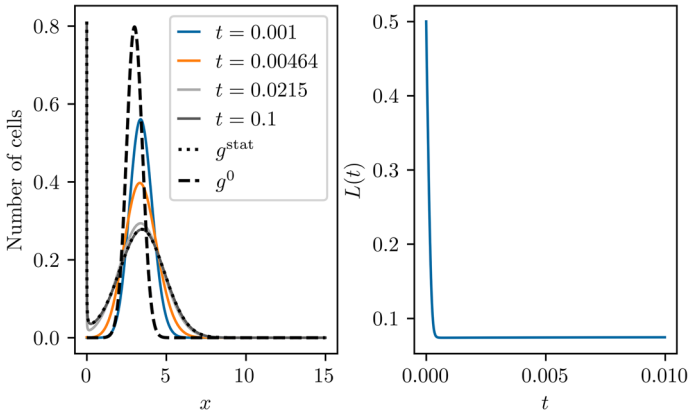

Fig. 5 On the left: time evolution of the size distribution with respect to size in the bimodal case; on the right: time evolution of the external lipid concentration. We observe that the asymptotic profile coincides with the computed stationary solution. Parameters of the system are given at Table 1

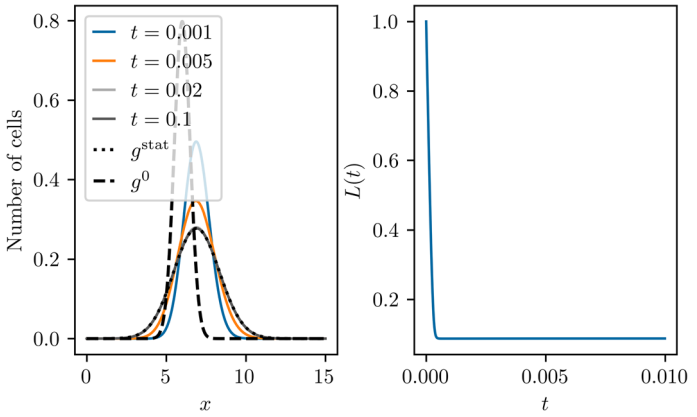

Fig. 6 On the left: distributions of adipocytes with respect to size, i.e. amount of lipids, starting with $\lambda = 7$ and initial distribution $g^0(x) = C \exp\left(-\frac{1}{2}\left(\frac{x-6}{0.5}\right)^2\right)$ (in dashed blue line). On the right: time evolution of the external lipid concentration. Asymptotic profile (dotted yellow line) and stationary solution (black full line) both present unimodality. Parameters of the system are given at Table 1 (color figure online)

and the initial amount of lipids λ are conserved, as expected. In Fig. 5, we plot the time evolution of the solution : on the left, adipocyte density is displayed as a function of x for various times and on the right, the evolution with respect to time of external lipid concentration L is plotted. We observe that L tends to a stationary value and g to a stationary profile with bimodality as expected.

Now we may investigate the behaviour of the stationary solutions and the asymptotic profiles with respect to λ. A first crucial information is that depending on λ, different types of modality can be observed. Figure 6 presents a case where the stationary solu-

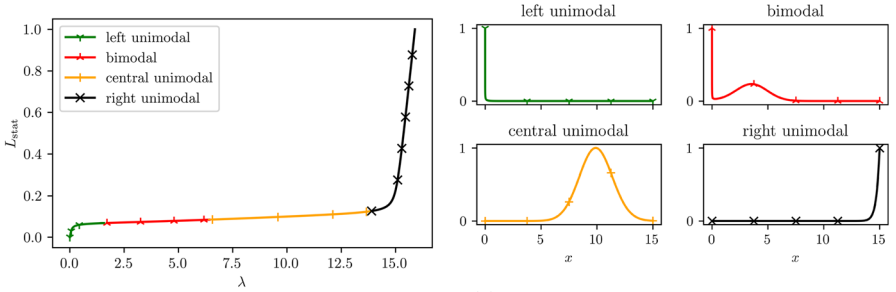

(a) $\phi^{-1}(\lambda)$

(b) Different types of modality for stationary solutions

Fig. 7 Different types of stationary solutions : on the left we plot the inverse of the function $\phi : L \to L + \int_0^\infty x M_L(x)\mathrm{d}x$. We plot the inverse ϕ^{-1} rather than ϕ because the value we change in the model is λ and not L^{stat}. Some points are colored according to the type of stationary solution we obtain. There are indeed four different types of stationary solutions: left unimodal (in green), bimodal (in red), central unimodal (in yellow) and right unimodal (in black). On the right: for each type, a stationary solution is plotted in the same color as on the left for one value of λ. Left unimodal (here for $\lambda = 0.191$) corresponds to the case where there is not enough lipids in the system and therefore all cells are of small size. Bimodal (here for $\lambda = 3.52$) is the expected behaviour of the stationary distribution with both small and large cells. Central unimodal (here for $\lambda = 9.96$) happens when the amount of lipids λ is too large and most cells are of large size. This is not observed *in vivo*, where we expect a little amount of small cells to remain. Right unimodal (here for $\lambda = 14.9$) happens when the total amount of lipids is very large and due to the null-flux boundary conditions most cells are of the maximal size $x_{\max} = 15$. This behaviour is not biologically relevant (color figure online)

tion is unimodal, obtained with initial conditions $g^0(x) = C \exp\left(-\frac{1}{2}\left(\frac{x-6}{0.5}\right)^2\right)$, where C is choosen such that $m = 1$, and L^0 such that $\lambda = 7$. We remark that L also tends to a stationary value and densities converge towards a stationary distribution with unimodality. Biologically, we can relate this to the fact that if the amount of lipids in the system is higher, cells have a tendency to put into storage the maximum amount of lipids and thus cells are bigger in average. From a mathematical point of view, since the optima can be linked to the velocity zeros, this means that for bigger λ, two of the zeros of speed V - and therefore two optima - disappear and thus only one zero remains giving rise to a unimodal profile.

More generally, we can investigate the profile modality with respect to the value of λ using the computation of stationary solutions. In Fig. 7 on the left, we present the type of modality of the stationary solutions as a function of λ. Left (resp. right) unimodality is labeled in green Y (resp. in black x) when a single mode concentrated on the left (resp. right) of the domain is observed. Central unimodal stationary solution is labeled in yellow + when the unique mode is concentrated inside the domain. Bimodality is labeled in red.

In Fig. 7 on the right, a plot for each of the 4 types of modality is presented. We represent the stationary solution $M_{L_{\text{stat}}}$ with respect to x. Four different values of L_{stat} corresponding to various λ are considered, namely $L_{\text{stat}} = 0.05$ and $\lambda = 0.191$ for the left unimodality (top left, in green), $L_{\text{stat}} = 0.075$ and $\lambda = 3.52$ for the bimodality (top right, in red), $L_{\text{stat}} = 0.1$ and $\lambda = 9.96$ for the central unimodality (bottom left, in

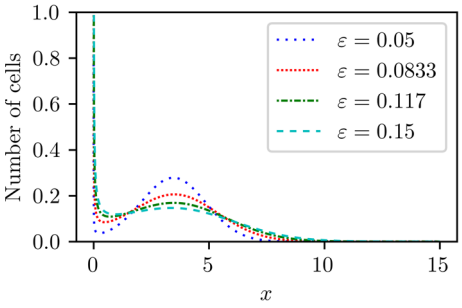

Fig. 8 Different stationary solutions depending on the value of ε. We observe that bimodality holds for values of ε small enough. Parameters of the system are given at Table 1

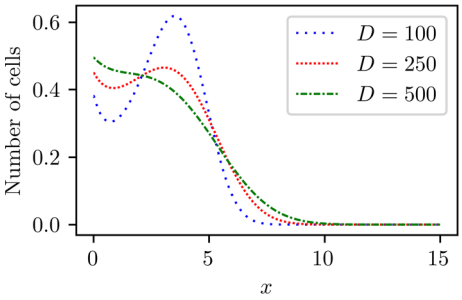

Fig. 9 Different stationary solutions depending on the value of diffusion rate D taken as constant in space and time. Parameters of the system are given at Table 1

yellow) and $L_{\text{stat}} = 0.2$ and $\lambda = 14.9$ for the right unimodality (bottom right, in black). For a biological interpretation, left modality is observed when the amount of lipids is too low and thus cells are of relative small sizes. Right modality is a consequence of the amount of lipids being too large and represents the whole cell population approaching its maximal volume. A mathematical interpretation is given by again considering the zeros of the velocity with an influence on the optima of the profile. Left (resp. right) modality is reached when zeros disappear and/or go outside the domain from the left (resp. from the right). The first mode in the bimodal case can also be localized at 0, the smallest zero of the velocity being outside the domain (on the left).

5.2.3 Influence of ε and comparison with a constant diffusion rate D

In this part, we explore the influence of parameter ε on the shape of stationary solutions. We can observe in Fig. 8 that higher values of ε smoothen the two maxima of the solution, as expected. For smaller values of ε, the nadir (i.e. the local minimum between the two maxima) gets sharper and for very small ε this may result numerically in taking very small time and space steps. This is easily interpreted as the fact that when $\varepsilon = 0$, we consider the classical Lifshitz–Slyozov system where stationary solutions are sums of Dirac masses which is difficult to obtain numerically without a dedicated scheme.

The choice we made for the diffusion rate is supported by the convergence results from the Becker–Döring to Lifshitz–Syozov model and the behaviour of second order terms. However this choice is not motivated by biological observation. Hence one may make the assumption that the diffusion rate is constant in both time and space. This unfortunately results in quite different results as shown in Fig. 9. We point out that to obtain bimodality some parameters need to be readjusted in this case. Hence

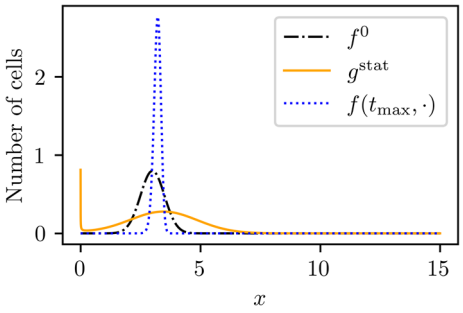

Fig. 10 Numerical solution for the first order Lifshitz–Slyozov model (11) (in dotted blue line) compared to the stationary solution of the Lifshitz–Slyozov diffusive model (18) (in orange plain line) with the same parameters and same initial condition (displayed in black dashed -dotted line). The solution to the first order Lifshitz–Slyozov model is expected to converge to a Dirac mass and is displayed for a time before reaching the asymptotic profile (color figure online)

comparing the solutions of the system under consideration (18) and the solutions with constant diffusion rate proves to be difficult because the behaviour of stationary solutions is heavily dependent on the choice of parameters.

We still can make a few comments about the resulting solutions. The constant diffusion rate tends to smoothen the first maximum whereas in the non-constant case, the diffusion is relatively close to zero, leading to a sharper maximum. Our investigation of the available data for adipose cell distribution leads us to believe that non-constant diffusion rates have better chances of making the model fit with the data. We also point out that in the case of constant diffusion, each type of modality, as previously described, is obtainable.

5.2.4 Comparison with the first order model

Stationary solutions for the first order Lifshitz–Slyozov model are not so easily computed theoretically. Nonetheless we can explore these solutions numerically as asymptotic profiles of the solutions of system (11). For that purpose, we use a standard upwind scheme for transport equations, since the velocity is known. Figure 10 presents the result of an upwind scheme for the Lifshitz–Slyozov model with the same initial conditions and parameters as in Fig. 5. We expect singular stationary state for the first order Lifshitz–Slyozov model. We may interpret stationary state that concentrates at two points as a degenerate bimodal solution. Using the same parameters as in Fig. 5, we can see on Fig. 11 that the solution concentrates to a singular Dirac mass and that in this case we cannot recover bimodality, unlike the case of second-order Lifshitz–Slyozov model, see Fig. 10. We also point out that the asymptotic values of L are different in both cases.

By changing initial conditions and the parameter β to $\beta = 100$, we can nonetheless obtain a bimodal solution for the first order Lifshitz–Slyozov model (11) as seen in Fig. 12 on the left. However, by changing the initial condition f^0, we can see on Fig. 12 on the right that we do not obtain the same asymptotic solutions. This leads us to believe that in the case of the first order Lifshitz–Slyozov model the asymptotic

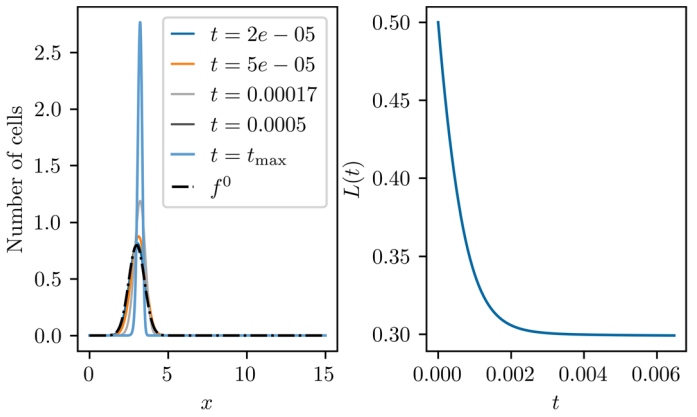

Fig. 11 Numerical solution for the first order Lifshitz–Slyozov model (11) with same parameters and initial data as in Fig. 5. On the left: time evolution of the size distribution with respect to size; on the right: time evolution of the external lipid concentration. The solution to the first order Lifshitz–Slyozov model is expected to converge to a Dirac mass and is displayed for a time before reaching the asymptotic profile

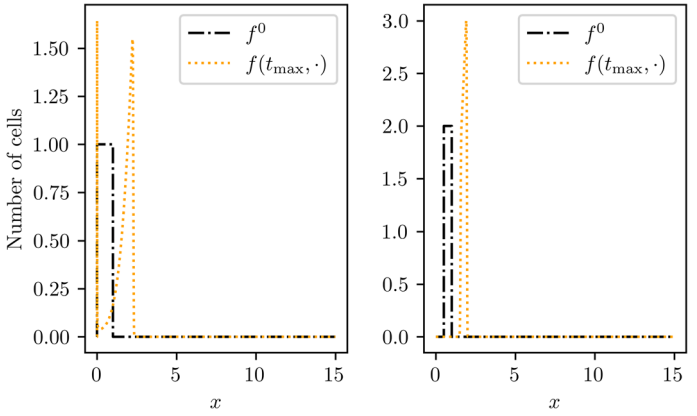

Fig. 12 Asymptotic profiles for the first order Lifshitz–Slyozov model (11) with $m = 1$ and $\lambda = 2$. Left: $f^0(x) = C\mathbb{1}_{[\Delta x,1]}(x)$. Right: $f^0(x) = C\mathbb{1}_{[0.5,1]}(x)$. The difference in the initial conditions leads to different profiles. To observe bimodality the parameter β was changed to $\beta = 100$ in both cases

solutions depend on the initial condition g^0 and not only on m and λ, unlike for second order Lifshitz–Slyozov model (18).

5.2.5 The case $\lambda < \Phi(0)$

As explained in the remark of Sec. 4.2, for different choices of functions a and b than those of the adipocyte model, we may find situations where $\lim_{L\to 0^+} \Phi(L) = \lambda_0 > 0$. In this subsection, we explore the evolution of a solution for a value of λ such that $0 < \lambda < \lambda_0$, that is to say in a case when no smooth stationary solution exists. An example of choice for a and b is $a(x) = 1$ and $b(x) = (x+1)^{2/3}$ and in Fig. 13, the function $L \to \Phi(L)$ is displayed in that case.

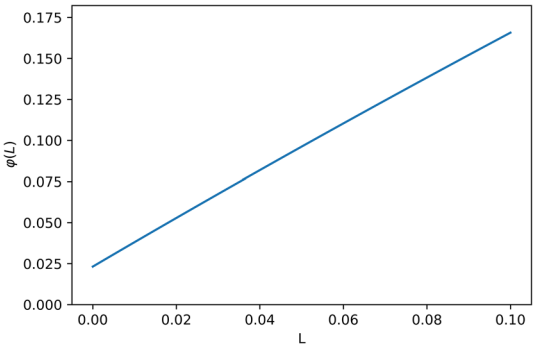

Fig. 13 Plot of function $L \to \Phi(L)$ with $a(x) = 1$ and $b(x) = (x+1)^{2/3}$. In that case, $\lim_{L\to 0^+} \Phi(L) \sim 0.025 > 0$ and the existence of smooth stationary solutions for values of λ such that $\lambda < \lambda_0$ is not guaranteed

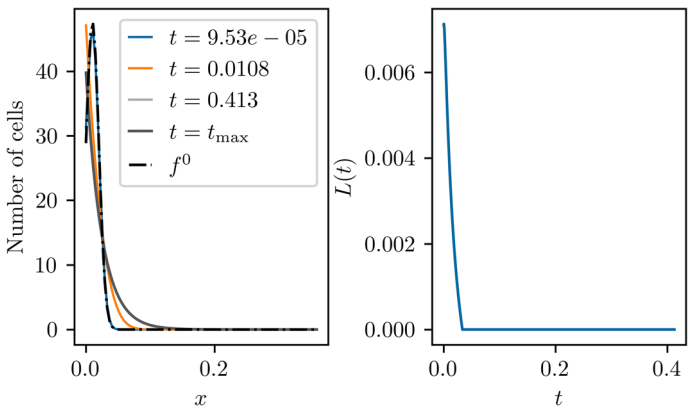

Fig. 14 Case when $a(x) = 1$ and $b(x) = (x+1)^{2/3}$ and $\lambda < \lambda_0$. On the left: time evolution of the size distribution with respect to size; on the right: time evolution of the external lipid concentration

We show in Fig. 14 the time evolution of the density profile (on the left) and of the external lipid concentration L (on the right) computed numerically in a case where $\lambda < \lambda_0$. We observe that, as expected, L tend to 0 asymptotically and that the adipocyte density seems to converge towards a Dirac mass centered at 0. Numerical simulations prove difficult because of the constraint on Δt to enforce the stability of the numerical scheme. More precisely, this constraint induces that Δt should be bounded above by L^n. Hence as the computation time increases, we observe that the value of L^n tends to zero, as the solution gets closer to the asymptotic profile and therefore that the time step eventually gets smaller than machine precision. In this case, the scheme fails to conserve both λ and m.

6 Conclusion

Our work provides a new approach for looking into convergence from Becker–Döring to Lifshitz–Slyozov, and numerical results indicating that the second order Lifshitz–Slyozov model is better suited to model adipocyte size distribution than previous approach relying on first order Lifshitz–Slyozov model.

The originality of this study lies in the following points :

- a new second order Lifshitz–Slyozov model (18) for adipocyte size distribution with a diffusion term derived from a discrete model,
- Becker–Döring and Lifshitz–Slyozov systems with an unusual velocity (46) -(5) with three zeros and a saturation term in L, which leads to different types of stationary solutions,
- an additional conservation law (8) with respect to classical systems, enforcing uncommon boundary conditions, see Eq. (10) and (17),
- a new proof of convergence result from Becker–Döring solutions to Lifshitz–Slyozov solutions, using tails of distributions, that provides an upper bound on the speed of convergence.
- numerical results showing that bimodal distributions, as well as unimodal profiles, can be obtained asymptotically with system (18), according to the parameters,
- numerical results exploring the influence of parameter ε and comparing the diffusion term of system (18) with a time and space constant coefficient.
- numerical results shows that the second order system (18) provides universal asymptotic profile that does not depend on initial condition (but only on λ, m), contrary to first order system (11).

We believe that the distribution tail approach could be further investigated to show convergence towards the solutions to the second order Lifshitz–Slyozov equation. The asymptotic behaviour of solutions to the second order Lifshitz–Slyozov model will be investigated in future works.

Annex: Compactly supported solution

We look at the solutions of

$$\begin{cases} \partial_t f(t,x) + \partial_x (v(x, L(t)) f(t,x)) = 0, & \text{(45a)} \\ L(t) + \displaystyle\int_{\mathbb{R}_+} x f(t,x) \mathrm{d}x = \lambda, & \text{(45b)} \\ (v(x, L(t)) f(t,x))\big|_{x=0} = 0, & \text{(45c)} \\ f(0,x) = f^0(x) \text{ and } L(0) = L^0, & \text{(45d)} \end{cases}$$

with

$$v(x, L) = a(x) \frac{L}{L + \kappa} - b(x). \tag{46}$$

We show the following lemma

Lemma 6.1 *Assume f^0 is a finite measure. Assume a and b are C^1 globally Lipschitz functions, and furthermore that a is bounded and b monotonously increasing from 0 to $+\infty$. Then if f^0 is compactly supported, the unique solution of (45) is compactly*

supported for all times, and there exists x^∞ such that

$$\lim_{t\to\infty} \int_x^\infty f(t,y)\mathrm{d}y \le \left(\int_0^\infty f^0(y)\mathrm{d}y\right) 1_{x\le x^\infty}. \tag{47}$$

Note that the assumptions on a and b are satisfied by (4)–(5).

Proof Well-posedness under smooth linearly bounded coefficients is granted, see for instance (Collet and Goudon 2000; Calvo et al. 2021). For the control of the support of its solution, we use the comparison principle for the tail distribution. Let K such that $a(x) \le K$ for all x, and let define g the solution of the *linear* transport equation

$$\begin{cases} \partial_t g(t,x) + \partial_x((K - b(x))g(t,x)) = 0, & \text{(48a)} \\ ((K - b(x)))g(t,x))\big|_{x=0} = 0, & \text{(48b)} \\ g(0,x) = f^0(x). & \text{(48c)} \end{cases}$$

Let $F(t,x) = \int_x^\infty f(t,y)\mathrm{d}y$ and $G(t,x) = \int_x^\infty g(t,y)\mathrm{d}y$. Using similar calculations as in the proof of Lemma 3.6, we easily obtain

$$\begin{aligned} &\partial_t(G-F)(t,x) + ((K-b(x))\partial_x(G-F)(t,x) \\ &= \left(a(x)\frac{L}{L+\kappa} - K\right)\partial_x F(t,x) \ge 0, \end{aligned} \tag{49}$$

so that we have for all times t and all x, by comparison principle (and because it holds true at time 0),

$$F(t,x) \le G(t,x). \tag{50}$$

The end of the proof follows by trivial calculation on the linear transport equation, with $x^\infty = b^{-1}(K)$. □

Data availibility The datasets generated during and/or analyzed during the current study are available from the corresponding author on reasonable request.

References

Arner P, Bernard S, Appelsved L, Fu K-Y, Andersson DP, Salehpour M, Thorell A, Rydén M, Spalding KL (2019) Adipose lipid turnover and long-term changes in body weight. Nat Med 25(9):1385–1389

Ball JM, Carr J, Penrose O (1986) The Becker–Döring cluster equations: basic properties and asymptotic behaviour of solutions. Commun Math Phys 104(4):657–692

Becker R, Döring W (1935) Kinetische behandlung der keimbildung in übersättigten dämpfen. Ann Phys 416(8):719–752

Cañizo JA, Einav A, Lods B (2019) Uniform moment propagation for the Becker–Döring equations. Proc R Soc Edinb: Sect A Math 149(04):995–1015

Calvez V, Lenuzza N, Doumic M, Deslys J-P, Mouthon F, Perthame B (2010) Prion dynamics with size dependency-strain phenomena. J Biol Dyn 4(1):28–42

Calvo J, Doumic M, Perthame B (2018) Long-time asymptotics for polymerization models. Commun Math Phys 363:111–137
Calvo J, Hingant E, Yvinec R (2021) The initial-boundary value problem for the Lifshitz–Slyozov equation with non-smooth rates at the boundary. Nonlinearity 34(4):1975
Collet J-F, Goudon T (2000) On solutions of the Lifshitz–Slyozov model. Nonlinearity 13(4):1239
Collet J-F, Goudon T, Vasseur A (2002) Some remarks on large-time asymptotic of the Lifshitz–Slyozov equations. J Stat Phys 108(1):341–359
Conlon JG, Schlichting A (2019) A non-local problem for the Fokker–Planck equation related to the Becker–Döring model. Discrete Contin Dyn Syst 39(4):1821–1889
Deschamps J, Hingant E, Yvinec R (2017) Quasi steady state approximation of the small clusters in Becker–Döring equations leads to boundary conditions in the Lifshitz–Slyozov limit. Commun Math Sci 15(5):1353–1384
Divoux A, Clement K (2011) Architecture and the extracellular matrix: the still unappreciated components of the adipose tissue. Obes Rev 12(5):e494–e503
Doumic M, Goudon T, Lepoutre T (2009) Scaling limit of a discrete prion dynamics model. Commun Math Sci 7(4):839–865
Giacobbi A-S, Meyer L, Ribot M, Yvinec R, Soula H, Audebert C (2023) Mathematical modeling of adipocyte size distributions: identifiability and parameter estimation from rat data
Gilleron J, Goudon T, Lagoutière F, Martin H, Mauroy B, Millet P, Ribot M, Vaghi C (2020) Modeling and analysis of adipocytes dynamic with a differentiation process. ESAIM: Proc Surv, 67:210–241
Goudon T, Monasse L (2020) Fokker–Planck approach of ostwald ripening: simulation of a modified Lifshitz–Slyozov–Wagner system with a diffusive correction. SIAM J Sci Comput 42(1):B157–B184
Greer ML, Pujo-Menjouet L, Webb GF (2006) A mathematical analysis of the dynamics of prion proliferation. J Theor Biol 242(3):598–606
Hariz S, Collet JF (1999) A modified version of the Lifshitz–Slyozov model. Appl Math Lett 12(1):81–85
Hingant E, Yvinec R (2017) Deterministic and stochastic Becker–Döring equations: past and recent mathematical developments. stochastic processes. Multiscale Modeling, and Numerical Methods for Computational Cellular Biology. Springer, Cham, pp 175–204
Jackson GA, Burd AB (1998) Aggregation in the marine environment. Environ Sci Technol 32(19):2805–2814
Jin S, Yan B (2011) A class of asymptotic-preserving schemes for the Fokker–Planck–Landau equation. J Comput Phys 230(17):6420–6437
Jo J, Gavrilova O, Pack S, Jou W, Mullen S, Sumner AE, Cushman SW, Periwal V (2009) Hypertrophy and/or hyperplasia: dynamics of adipose tissue growth. PLoS Comput Biol 5(3):e1000324
Jo J, Shreif Z, Gaillard JR, Arroyo M, Cushman SW, Periwal V (2015) Mathematical models of adipose tissue dynamics. The Mechanobiology of Obesity and Related Diseases, pp 11–34
Jo J, Shreif Z, Periwal V (2012) Quantitative dynamics of adipose cells. Adipocyte 1(2):80–88
Kim J, Saidel GM, Kalhan SC (2008) A computational model of adipose tissue metabolism: evidence for intracellular compartmentation and differential activation of lipases. J Theor Biol 251(3):523–540
Laurençot P (2001) Weak solutions to the Lifshitz–Slyozov–Wagner equation. Indiana Univ Math J 50(3):1319–1346
Laurençot P, Mischler S (2002) From the Becker–Döring to the Lifshitz–Slyozov–Wagner equations. J Stat Phys 106(5):957–991
Laurençot P, Walker C (2007) Well-posedness for a model of prion proliferation dynamics. J Evol Equ 7(2):241–264
Lee KY, Luong Q, Sharma R, Dreyfuss JM, Ussar S, Kahn CR (2019) Developmental and functional heterogeneity of white adipocytes within a single fat depot. EMBO J 38(3):e99291
Lifshitz IM, Slyozov VV (1961) The kinetics of precipitation from supersaturated solid solutions. J Phys Chem Solids 19(1):35–50
Niethammer B (2004) Macroscopic limits of the Becker–Döring equations. Commun Math Sci 2:85–92
Niethammer B, Pego RL (1999) Non-self-similar behavior in the LSW theory of Ostwald ripening. J Stat Phys 95:867–902
Penrose O, Lebowitz JL, Marro J, Kalos MH, Sur A (1978) Growth of clusters in a first-order phase transition. J Stat Phys 19:243–267
Peurichard D, Delebecque F, Lorsignol A, Barreau C, Rouquette J, Descombes X, Casteilla L, Degond P (2017) Simple mechanical cues could explain adipose tissue morphology. J Theor Biol 429:61–81

Peurichard D, Ousset M, Paupert J, Aymard B, Lorsignol A, Casteilla L, Degond P (2019) Extra-cellular matrix rigidity may dictate the fate of injury outcome. J Theor Biol 469:127–136
Prana V, Tieri P, Palumbo MC, Mancini E, Castiglione F (2019) Modeling the effect of high calorie diet on the interplay between adipose tissue, inflammation, and diabetes. Computational and Mathematical Methods in Medicine, 2019
Prigent S, Ballesta A, Charles F, Lenuzza N, Gabriel P, Tine LM, Rezaei H, Doumic M (2012) An efficient kinetic model for assemblies of amyloid fibrils and its application to polyglutamine aggregation. PLoS ONE 7(11):e43273
Schlichting A (2019) Macroscopic limit of the Becker–Döring equation via gradient flows. ESAIM: Control Optim Calculus Var, 25:22
Simonett G, Walker C (2006) On the solvability of a mathematical model for prion proliferation. J Math Anal Appl 324(1):580–603
Soula HA, Geloen A, Soulage CO (2015) Model of adipose tissue cellularity dynamics during food restriction. J Theor Biol 364:189–196
Soula HA, Julienne H, Soulage CO, Geloen A (2013) Modelling adipocytes size distribution. J Theor Biol 332:89–95
Varlamov O, Somwar R, Cornea A, Kievit P, Grove KL, Roberts CT Jr (2010) Single-cell analysis of insulin-regulated fatty acid uptake in adipocytes. Am J Physiol-Endocrinol Metab 299(3):E486–E496
Vasseur A, Poupaud F, Collet J-F, Goudon T (2002) The Beker–Döring system and its Lifshitz–Slyozov limit. SIAM J Appl Math 62(5):1488–1500
Wurl O, Wurl E, Miller L, Johnson K, Vagle S (2011) Formation and global distribution of sea-surface microlayers. Biogeosciences 8(1):121–135